ResearchGate

See discussions, stats, and author profiles for this publication at: https://www.researchgate.net/publication/363995426

Neurocognitive predictors of food memory in healthy adults – a preregistered analysis

Preprint · September 2022

DOI: 10.13140/RG.2.2.25794.45767

CITATIONS
0

READS
127

5 authors, including:

Ronja Thieleking
Max Planck Institute for Human Cognitive and Brain Sciences
23 PUBLICATIONS **29** CITATIONS
SEE PROFILE

Evelyn Medawar
Max Planck Institute for Human Cognitive and Brain Sciences
40 PUBLICATIONS **261** CITATIONS
SEE PROFILE

Arno Villringer
Max Planck Institute for Human Cognitive and Brain Sciences
1,315 PUBLICATIONS **48,219** CITATIONS
SEE PROFILE

Veronica Witte
University of Leipzig Medical Center and Max Planck Institute for Human Cognitive a…
232 PUBLICATIONS **4,964** CITATIONS
SEE PROFILE

Some of the authors of this publication are also working on these related projects:

The use of resting-state functional MRI for assessing cerebral perfusion in acute ischemic stroke View project

Training of Working memory functions View project

All content following this page was uploaded by Ronja Thieleking on 29 September 2022.

The user has requested enhancement of the downloaded file.

Neurocognitive predictors of food memory in healthy adults – a preregistered analysis

Neurocognitive predictors of food memory

Thieleking, Ronja[1], Medawar, Evelyn[1], Villringer, Arno[1,2], Beyer, Frauke[1,2], Witte, A.Veronica[1,2]

[1]Max Planck Institute for Human Cognitive Behaviour and Brain Sciences, 04103 Leipzig, Germany

[2]Cognitive Neurology, University of Leipzig Medical Center, 04103 Leipzig, Germany

Corresponding author:

Veronica Witte: witte@cbs.mpg.de

Contributions of authors:

RT: Designed research, Performed research, Analyzed data, Wrote the paper

EM: Designed research, Performed research

FB: Analyzed data

AV: Designed research

VW: Designed research, Wrote the paper

Number of pages: 50

Number of figures: 15

Number of tables: 3

Number of words for abstract, introduction, and discussion (separately):

abstract: 233 words

introduction: 650 words

discussion: 1499 words

Conflict of interest statement: The authors declare no competing financial interests.

Acknowledgments: I am very thankful to Anne-Katrin Brecht, Larissa de Biasi, Leonie Disch, Lina Eisenberg, Laura Hesse, Niklas Hlubek, Lynn Mosesku, Lukas Recker, Lennard Schneidewind, Emira Shehabi, Hannah Stock, Christian Schneider, Emmy Töws, Anna-Luisa Wehle, Charlotte Wiegank and Marie Zedler who were involved in the recruitment of participants, collecting data on test days as well as helping with organizing and preprocessing the huge amount of very diverse data that we collected for the overarching project. I also would like to thank Stephen Granger who was of great help with the tractography software and in deciding on the regions of interest for tractography of the uncinate fasciculus. I am also thankful to Tilman Stephani for reviewing the immense amount of code which I scripted for this analysis and thereby contributing to significant improvements of the code.

Index

I Abstract

Memory processes have long been known to determine food choices(Rozin and Zellner, 1985) but recognition memory of food and its cognitive, homeostatic and neuroanatomical predictors are still largely understudied.

60 healthy, overweight, non-restricted eating adults (20 females) took part in a food wanting and subsequent food recognition and lure discrimination 3T-fMRI tasks at four time points after a standardized breakfast shake. With advanced tractography of diffusion-weighted imaging data, we investigated the influence of the uncinate fasciculus' (UF) brain microstructure on the interplay of food wanting and memory processes. The analysis was preregistered in detail and conducted with Bayesian multilevel regression modeling.

Target recognition (d') and lure discrimination (LDI) performance of food was higher than of art images. On the single item level (but not per wanting category), wanting enhanced recognition accuracy. This enhancement by reward anticipation was most pronounced during memory encoding. Subjective hunger level did not predict performance on the memory task. The microstructure of the UF did neither evidently affect memory performance outcomes nor moderate the wanting enhancement of the recognition accuracy.

We shed light on a to date understudied process in food decision-making: reward anticipation influenced food recognition accuracy which in turn shapes food decisions. Due the undetected role of brain microstructure in food decision processes in our study population, we suggest extending investigation of this interplay to brain activity as well as to populations with eating behaviour disorders.

II Significance Statement

In times of pandemic overnutrition, disadvantageous food choices need to be understood to attenuate

excessive calorie intake. Memory processes influence food choices but food recognition memory remains understudied. We shed light on the interplay of food memory and food wanting underpinned by magnetic resonance imaging and advanced brain tractography. We discovered that higher food wanting led to better recognition accuracy revealing a to date disregarded process in food decision-making. However, we could not detect a moderating role of the white matter tract connecting reward and memory brain areas. We are confident about the detected effects as we applied Bayesian statistics with low false positives rates. We additionally aimed to reduce publication bias through detailed preregistration of our study and analysis.

III Introduction

In a world overloaded with food stimuli, cognitive processes contributing to food choices move into focus, especially considering public health strategies to address the overnutrition pandemic(Berthoud, 2012). The complexity of food choices reflects in current debates around food desires (wanting) (García-García et al., 2020) and food memory(Seitz et al., 2021b). Well-known memory processes crucial for food choices represent previously learned preferences(Rozin and Zellner, 1985). Recently, memory of eating(Higgs and Spetter, 2018; Seitz et al., 2021a), working memory (Spetter et al., 2020) and spatial food memory(de Vries et al., 2020) have been established as modifiers of food intake. Largely understudied though is the role of recognition memory in food choices. Both, food recognition memory and food choices are constantly manipulated by the daily overload of food stimuli. Additionally, metabolic hunger impacts food choices, namely food wanting(Berthoud, 2007), and food memory(Morris and Dolan, 2001). We aim to shed light on how food wanting and hunger determine food memory and how the underlying neural anatomy contributes to this interplay.

The importance of the hippocampus in memory(Wixted and Squire, 2010) and the regulation of human food intake has been extensively studied, e.g. its inhibitory output to hypothalamic feeding centers(see

review by Stevenson and Francis, 2017). However, modulation of food memory through cognitive processes and associated neural pathways providing input to the hippocampus are mostly understudied. Modulatory input to the hippocampus provides the amygdala—directly as well as indirectly through the entorhinal cortex(Kensinger and Schacter, 2006; Roesler and McGaugh, 2022). The amygdala and the orbito-frontal cortex (OFC) are implicated in the encoding of (food) value(Canli et al., 2000; Richardson et al., 2004; Warlow and Berridge, 2021) and in hunger enhanced recognition memory(Morris and Dolan, 2001). Nevertheless, the influence of subjective food value, namely food wanting, on recognition memory as well as the contribution of the underlying neural pathways remain unclear.

The neural pathway connecting the OFC with the amygdala and entorhinal cortex is the uncinate fasciculus (UF)(Thiebaut de Schotten et al., 2012; Von Der Heide et al., 2013). The microstructural coherence of the UF correlates with emotional memory(Yau et al., 2009) and emotion management(Pisner et al., 2017) as well as with activation of the hippocampus during an emotional memory task(Granger et al., 2021). As emotions and subjective value are processed in the same brain areas (OFC(Gottfried et al., 2003) and amygdala(Murray, 2007)), we hypothesized a putative top-down modulatory control by microstructural properties of the UF in memory processes which integrate food wanting and hunger.

Besides recognition of food items, the ability to detect differences in visual details (lure discrimination) form crucial parts of food memory and might influence food choices. Previous studies have revealed effects of emotion on both recognition and lure discrimination performance(Kensinger, 2007; Chainay et al., 2012; Leal et al., 2014) endorsing our assumption that parallelly processed reward reflected in food wanting might also affect food memory. To study the influence of reward on memory, we contrasted art to food images as art images can elicit similar desire and reward patterns in the

brain(Berridge and Kringelbach, 2008).

Based on previous findings and our assumptions, we formulated the following research questions:

1. Is the recognition performance for food items better than for non-food (art) items?
2. Does subjective hunger level modulate recognition performance for food items?
3. Could the recognition performance for food items (or in general) be enhanced by wanting?
4. Does the coherence of the UF influence food recognition performance or any of the above mentioned correlations and modulations? Might only the coherence of a sub-bundle of the uncinate fasciculus be relevant for the information transmission?
5. Are these possible correlations and modulations comparable regarding discrimination of visual details?

To this end, we analyzed food wanting and memory performance, brain microstructure using diffusion-weighted magnetic resonance imaging (MRI) and subjective hunger level assessed during MRI in a well-characterized adult sample following a detailed preregistration at https://osf.io/2z4dn.

IV Methodology

IV.1 Experimental Design and Participants

The over-arching study was designed as a double-blind randomized controlled cross-over (within-subject) intervention trial and preregistered at https://osf.io/f6qz5. The detailed analysis for the present investigation whether wanting, subjective hunger and UF microstructure predict recognition performance and lure discrimination of food items was preregistered at https://osf.io/2z4dn. For this preregistered analysis, we evaluated data from all four time points cross-sectionally by controlling for possible intervention effects, so that we were able to feed n=181 data sets into the behavioural analysis and n=176 data sets into the neuroimaging analysis.

Each participant was invited four times to undergo extensive testing following identical procedures each time: fasted overnight, blood sampling (i.a. fasted ghrelin), anthropometric measurements (body mass index (BMI), fat mass (FM), Waist-to-Hip ratio (WHR)), standardized breakfast shake (10% of gender-individual calorie need based on Harris and Benedict(1918)), MR scanning including two fMRI tasks (with different picture sets for each visit), structural and diffusion-weighted imaging, and post-MRI computer tasks. All participants were reimbursed for participation and gave written informed consent. The study was approved by the Research Ethics Committee of the University of Leipzig and was conducted in accordance with the Declaration of Helsinki. Inclusion and exclusion criteria were predefined and registered at https://clinicaltrials.gov/ct2/show/NCT03829189. The study population consisted of 60 healthy adults (20 females), aged 19 to 45 years, with a BMI of 25 to 30 kg/m^2 at baseline visits. Female participants were required to take contraceptives to minimize hormonal variations induced by the menstrual cycle. Participants were excluded if they suffered from a neurological, psychiatric, or metabolic disorder or if they took any medication acting on the central nervous system. Also, pregnancy or lactation and any type of dietary restrictions or antibiotic treatment

in the last 3 months led to exclusion. For more details see the clinicaltrials.gov-preregistration. The study population can be described as young, healthy and overweight. At the beginning of each testing day, participants received a bioelectric impedance analysis to assess fat mass (FM) and their Waist-to-Hip ratio (WHR) was measured. In addition, we assessed participants' eating behaviour with the German versions of the TFEQ(Pudel and Westenhöfer, 1989) and EDEQ(Hilbert et al., 2007), socio-economic status(Lampert et al., 2013), personality traits with the NEO-Five-Factor-Inventory by Costa and McCrae(Borkenau and Ostendorf, 2008) and attention network performance(Fan et al., 2002).

IV.2 Imaging data collection

Magnetic resonance imaging (MRI) was conducted at a 3 Tesla Prisma Fit Magnetom (Siemens, Erlangen, Germany). Anatomical MRI was acquired using a T1-weighted MPRAGE sequence using the ADNI protocol with the following parameters: TR = 2300ms; TE = 2.98ms; flip angle = 9°; FOV: $(256\ mm)^2$; voxel size: $(1.0mm)^3$; 176 slices. Diffusion-weighted MRI data was acquired using the following parameters: TR = 5200ms; TE = 75ms; flip angle = 90°; FOV: $(220\ mm)^2$; voxel size: (1.7mm)3; 88 slices; max. b=1000 s/mm^2 in 60 diffusion directions (+ 7 b0-images); partial Fourier=7/8; GRAPPA-factor = 2; interpolation = OFF. Ap/pa-encoded b0-images were acquired for distortion correction.

DWI data were preprocessed following a high standard pipeline which includes denoising, removal of Gibbs-ringing artefact to increase image quality(Thieleking et al., 2021), correction for susceptibility distortions as well as correction for head motion and eddy currents. Quality control led to exclusion of four data sets as can be followed up on in the preregistration (https://osf.io/2z4dn). After quality assurance, we used model-free fiber reconstruction based on generalized q-sampling (GQI)(Yeh et al., 2010) to create in-vivo whole-brain normalized quantitative anisotropy (nQA) maps. This model-free

method, in comparison to a tensor-based approach, calculates spin distribution functions which presumably improve the modeling of crossing fibers and resolve partial volume effects and thereby result in more accurate deterministic tractography(Yeh et al., 2013). Next, we conducted deterministic diffusion tractography with DSI Studio (version 2022.01.11)(Yeh, 2021) and extracted mean normalized quantitative anisotropy values (nQA) of the UF as well as of a sub-bundle. Normalization of QA was performed by scaling the subject-wise maximum QA value to 1. All (pre)processing steps, tractography settings and regions of interest can be accessed in detail via GitLab (https://gitlab.gwdg.de/gut_brain_study/analysis_dsistudio_tractography).

IV.3 Behavioural assessment

Participants took part in a food wanting and subsequent food memory task. In both tasks, food was contrasted to art images. Food pictures, including nutrient values such as calorie content, were taken from the food-pics database(Blechert et al., 2014; Medawar et al., 2022), and the art.pics database(Thieleking et al., 2020) served as source for the art images. The wanting task included 80 food (20 per calorie quartile) and 80 art images (10 per art style). Food and art served as image category in the analysis. Participants indicated food and art wanting on an 8-point-Lickert scale (see Fig. 1) and, in order to stimulate reward anticipation, they received the highest-rated food item to eat and art image as print-out after scanning. For the statistical analysis, images were categorized into “unwanted”, “neutral” and “wanted” images based on the participants’ ratings. The wanting task represented the memory encoding phase and was followed by the memory task after a break of about 20mins with structural scans. The memory task also consisted of 80 food and 80 art images with 30 old (targets), 30 similar (lures) and 20 new images (novels) in each image category. The memory task was a combined recognition and lure discrimination task with corrected target recognition *d’*, lure discrimination index *LDI* and response accuracy as outcome measures. Participants had to indicate as

quickly as possible if they had seen the presented food or art image in the previous task (“old”), if they had not seen it before (“new”) or if it was similar to a previously seen image (“similar”) (see Fig. 1). No feedback on performance was provided. Wanting ratings for new and similar images were obtained after the MRI scan, meaning not during memory encoding. Nevertheless, wanting attribution occurred before the reward hand-out and was therefore similarly reward-anticipatory as for the old images.

Detailed calculation of the memory outcome measures d’ and LDI as well as the creation of the wanting categories can be followed up in the ReadMe under https://gitlab.gwdg.de/gut_brain_study/analysis_r_memory.

Before and after each of the fMRI tasks, participants were asked to indicate their hunger level on an 8-point-Lickert scale (‘How hungry are you right now?’ - 'not at all’ to ‘extremely hungry’). After the MR scanning, participants filled out an 8-point visual analogue scale to indicate their well-being regarding anxiety, nausea, exhaustion by and difficulty of the tasks. At the end of the study, participants additionally indicated liking ratings on all images that had been presented during the fMRI tasks. In order to assess general preference and not wanting, participants did not receive rewards after completion of the liking task.

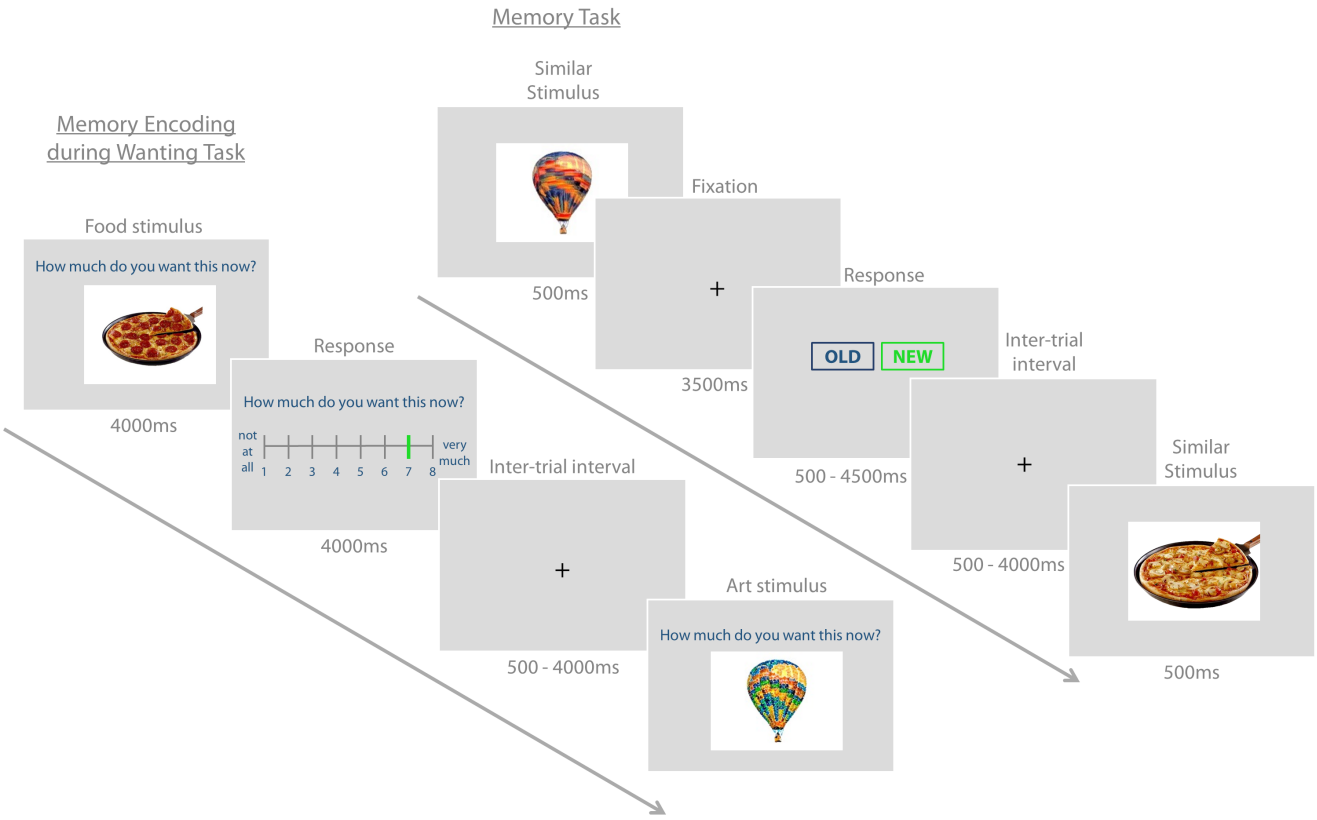

Figure 1: Wanting task and subsequent Memory task. Left: Memory Encoding during Wanting Task*: Participants were asked to indicate on an 8-point-Lickert scale how much they want to have the depicted food or art image. They were previously told that they would be rewarded with the highest rated food and art image after the MRI scan.* ***Right: Memory task including target recognition and lure discrimination****: Participants had to indicate as quickly as possible if they had seen the presented food or art image in the previous task ("old"), if they had not seen it before ("new") or if it was similar to a previously seen image (also "new"). Depicted are two exemplary similar (bot not identical) food and art stimuli.*

IV.4 Statistical Analysis

We applied Bayesian multilevel regression modeling as test statistic with R (version 4.1.1(R Core Team, 2021)). To assess the predictive accuracy of a Bayesian regression model (BRM), Vehtari,

Gelman, and Gabry proposed the expected log pointwise predictive density (elpd)(Vehtari et al., 2017) which can be estimated by leave-one-out (loo) cross-validation. The higher the predictive accuracy of a model, the higher is its elpd. We previously tested for random intercepts and random slopes present in the data, set up full models with these random effects and subsequently defined null models to test for fixed effects(van Doorn et al., 2021). As Bayesian inference testing is more conservative than classical comparison procedures that are based on Type I error, there is no need for multiple comparison testing(Gelman and Tuerlinckx, 2000).

In the result section, I present which Bayesian multilevel regression models (BRMs) predict the collected data most accurately and which effects we can therefore assume to exist in our study population. During Bayesian regression modeling, posterior distributions of the predictor variables are calculated. The mean estimate or the odds ratio and their 95%-credible interval (CI) of the posterior distributions result from this modeling. If the credible interval does not include Zero, we can infer that the effect is probably present in the study population. Through comparison of the predictive accuracy (elpd) of the full and null models, we can additionally find out which model predicts the data best. To follow-up on the model estimates of the predictors and random effects, tables were linked to the respective figures.

IV.5 Code accessibility

We version-controlled and published the tractography of white matter and the statistical analysis including details on software, functions and options via GitLab (REF). Regarding the tractography, all (pre)processing steps, settings and regions of interest can be accessed in detail here: (https://gitlab.gwdg.de/gut_brain_study/analysis_dsistudio_tractography). The code for the statistical analysis and all model results can be accessed here:

https://gitlab.gwdg.de/gut_brain_study/analysis_r_memory.

The code was checked for validity by a researcher who is independent of the study and the group and who has experience in using R.

V Results

V.1 Is the recognition performance for food items better than for non-food (art) items?

The corrected target recognition *d'* and the lure discrimination *LDI* are both higher for food compared to art (non-food = NF) images. The difference in memory indices between image categories was evident as the posterior distributions of the estimates revealed (Fig. 2). The comparison of the full models (Table 1, Eq. 1) with the null models (Table 1, Eq. 2) regarding predictive accuracy (expected log pointwise predictive density = elpd) is not conclusive though, due to larger standard errors than difference in predictive accuracy (Δelpd). Nevertheless, the certainty of the estimates, reflected in the credible intervals which do not include Zero, assures the difference in memory performance between image categories. Estimates of all predictors and covariates can be followed up in (Fig. 2-1, Tables 2-1 & 2-2).

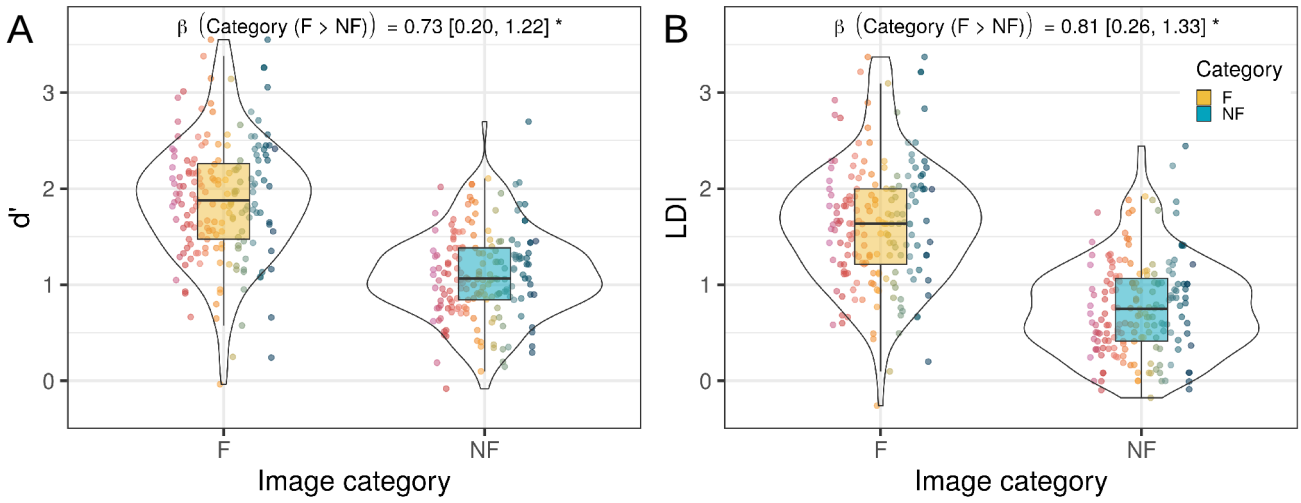

Figure 2: Memory performance per Image Category. A) The target recognition d' and B) the lure discrimination LDI of food (F) items *(yellow)* ***is better than of non-food (NF)/art items*** *(blue). Violin plots present the distribution of the two indices over the color-coded single subjects per image category. The estimate's CI did not include 0 which indicated an*

evident difference between image categories regarding d' and LDI. Estimates of all predictors and covariates are listed in Fig. 2-1 and Tables 2-1 & 2-2.

Table 1: Model equations of full and null models and the difference in predictive accuracy.

Eq. No.	Model Title	Model type	Model Equation dependent variable ~ predictors & covariates (without random effects for visual clarity)	Difference in Predictive Accuracy (Δelpd ± se)
1	**Category**	full model	d' / LDI ~ Image Category + Age + Gender + Intervention + Timepoint + Intervention*Timepoint	d': -0.1 ± 0.5 LDI: reference elpd
2	**Category**	null model	d' / LDI ~ Age + Gender + Intervention + Timepoint + Intervention*Timepoint	d': reference elpd LDI: -0.2 ± 0.5
3	**Complexity**	full model	Response accuracy ~ Image Category + normed Complexity + Image Category*normed Complexity + Wanting + Image Status + Gender + Age + Intervention + Timepoint + Intervention*Timepoint	response accuracy: -0.5 ± 1.1
4	**Complexity**	null model 1	Response accuracy ~ Image Category + normed Complexity + Wanting + Image Status + Gender + Age + Intervention + Timepoint + Intervention*Timepoint	response accuracy: reference elpd
5	**Complexity**	null model 2	Response accuracy ~ Image Category + Wanting + Image Status + Gender + Age + Intervention + Timepoint + Intervention*Timepoint	response accuracy: -0.8 ± 1.3
6	**Hunger**	full model	d' / LDI ~ Image Category + Subj Hunger Level + Image Category*Subj Hunger Level + Age + Gender + Intervention + Timepoint + Intervention*Timepoint	d': -2.8 ± 0.6 LDI: -1.9 ± 0.5
7	**Hunger**	null model 1	d' / LDI ~ Image Category + Subj Hunger Level + Age + Gender + Intervention + Timepoint + Intervention*Timepoint	d': -1.2 ± 0.5 LDI: -0.5 ± 0.4
8	**Hunger**	null model 2	d' / LDI ~ Image Category + Age + Gender + Intervention + Timepoint + Intervention*Timepoint	d': evidently highest elpd LDI: evidently highest elpd
9	**Wanting**	full model	d' / LDI ~ Image Category + Wanting Category + Image Category*Wanting Category + Age + Gender + Intervention + Timepoint + Intervention*Timepoint	d': -1.1 ± 1.2 LDI: -3.0 ± 1.5
10	**Wanting**	null model 1	d' / LDI ~ Image Category + Wanting Category + Age + Gender + Intervention + Timepoint + Intervention*Timepoint	d': reference elpd LDI: -1.7 ± 0.8
11	**Wanting**	null model 2	d' / LDI ~ Image Category + Age + Gender + Intervention + Timepoint + Intervention*Timepoint	d': -0.2 ± 2.0 LDI: evidently highest elpd
12	**Single item wanting**	full model	Response accuracy ~ Image Category + Wanting + Image Category*Wanting + Image Status + Age + Gender + Intervention + Timepoint + Intervention*Timepoint	response accuracy: evidently highest elpd
13	**Single item wanting**	null model 1	Response accuracy ~ Image Category + Wanting + Image Status + Age + Gender + Intervention + Timepoint + Intervention*Timepoint	response accuracy: -2.7 ± 2.0
14	**Single item wanting**	null model 2	Response accuracy ~ Image Category + Image Status + Age + Gender + Intervention + Timepoint + Intervention*Timepoint	response accuracy: -8.5 ± 3.8
15	**Image Status**	full model	Response accuracy ~ Image Category + Wanting + Image Status + Image Category*Wanting + Image Status*Wanting + Image Status*Image Category + Age + Gender + Intervention + Timepoint + Intervention*Timepoint	response accuracy: reference elpd
16	**Image Status**	null model 1	Response accuracy ~ Image Category + Wanting + Image Status + Image Category*Wanting + Image Status*Wanting + Age + Gender + Intervention + Timepoint + Intervention*Timepoint	response accuracy: -1.3 ± 1.4
17	**Image Status**	null model 2	Response accuracy ~ Image Category + Wanting + Image Status + Image Category*Wanting + Age + Gender + Intervention + Timepoint + Intervention*Timepoint	response accuracy: -7.8 ± 4.5
18	**Image Status**	null model 3	Response accuracy ~ Image Category + Wanting + Image Status+ Age + Gender + Intervention + Timepoint + Intervention*Timepoint	response accuracy: -10.5 ± 4.9
19	**UF**	full model	d' / LDI ~ Image Category + Wanting Category + Subj Hunger Level + nQA(UF) + Image Category*nQA(UF) + Wanting Category*nQA(UF) + Subj Hunger Level*nQA(UF) + Age + Gender + Intervention + Timepoint + Intervention*Timepoint	d' : -1.1 ± 2.5 LDI: -4.3 ± 1.9
20	**UF**	null model 7	d' / LDI ~ Image Category + Wanting Category + Subj Hunger Level + nQA(UF) + Age + Gender + Intervention + Timepoint + Intervention*Timepoint	d': -1.7 ± 0.5 LDI: -3.1 ± 1.1
21	**UF**	null model 11	d' / LDI ~ Image Category + nQA(UF) + Age + Gender + Intervention + Timepoint + Intervention*Timepoint	d': -1.2 ± 2.0 LDI: -0.6 ± 0.6
22	**UF**	null model 13	d' / LDI ~ Image Category + Wanting Category + Age + Gender + Intervention + Timepoint + Intervention*Timepoint	d': reference elpd LDI: -1.5 ± 1.0
23	**UF**	null model 14	d' / LDI ~ Image Category + Age + Gender + Intervention + Timepoint + Intervention*Timepoint	d': -0.6 ± 2.0 LDI: reference elpd

V.1.a Does the complexity of the single images influence response accuracy? (exploratory)

The complexity of the food (F) and art (NF) images might partly explain the higher response accuracy for food items as the complexity of the food images is in general lower than of the art images (Fig. 3 A) whereas other image characteristics were not different (arousal, recognizability and valence). However, the effect of higher response accuracy due to lower complexity might be restricted to food images reflected in the evident interaction effect (Fig. 3 B & Fig. 3-1). Nonetheless, the model comparison (model equations see Table 1, Eq. 3-5) does not allow for conclusions (Table 3-1) and no inference can

be drawn on the general role of complexity for response accuracy.

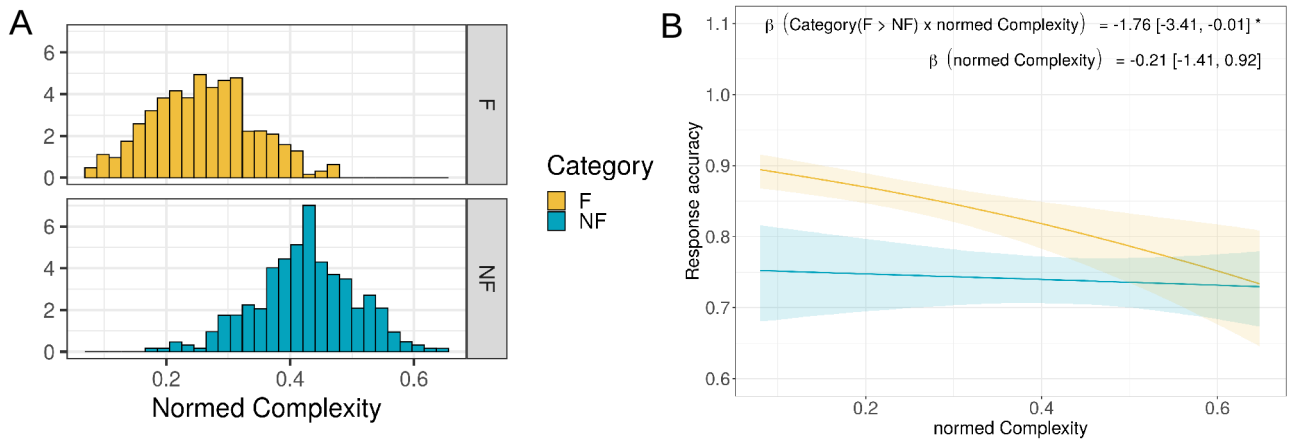

Figure 3: Normed complexity of food and art images. *A) Normed Complexity values are not equally distributed over the two image categories. Non-Food (art) images have on average a higher normed complexity than food images. B) Response accuracy depending on normed complexity of the images.* ***Image complexity might predict response accuracy of food items.*** *The estimate of the interaction of the full model (Table 1, Eq. 3) indicated that the response accuracy of the two image categories was differently affected by normed complexity, namely food stronger than art images. Odds ratios of all predictors and covariates are listed in Fig. 3-1 and Table 3-1.*

V.2 Does subjective hunger level moderate recognition or lure discrimination performance for food items?

The mean subjective hunger level averaged across MRI session did not influence food recognition (Fig. 4 A) nor lure discrimination performance (Fig. 4 B). Subjective hunger level neither had an effect on art (NF) memory performance (Fig. 4 B) nor independently of image category (Fig. 4-1). The lack of an effect of subjective hunger could also be inferred from the model comparison as the null model 2 without subjective hunger as predictor evidently showed the highest predictive accuracy for *d'* and *LDI* (Table 1, Eq. 6-8; Tables 4-1 & 4-2). The irrelevance of subjective hunger is also visualized in the posterior distributions of the mean estimates (Fig. 4-2). As preregistered, we investigated if task-

specific subjective hunger level, i.e. during the wanting or memory task respectively, predicted (food) memory performance measures (Fig. 4-3). None of these task-specific hunger levels did influence target recognition or lure discrimination performance.

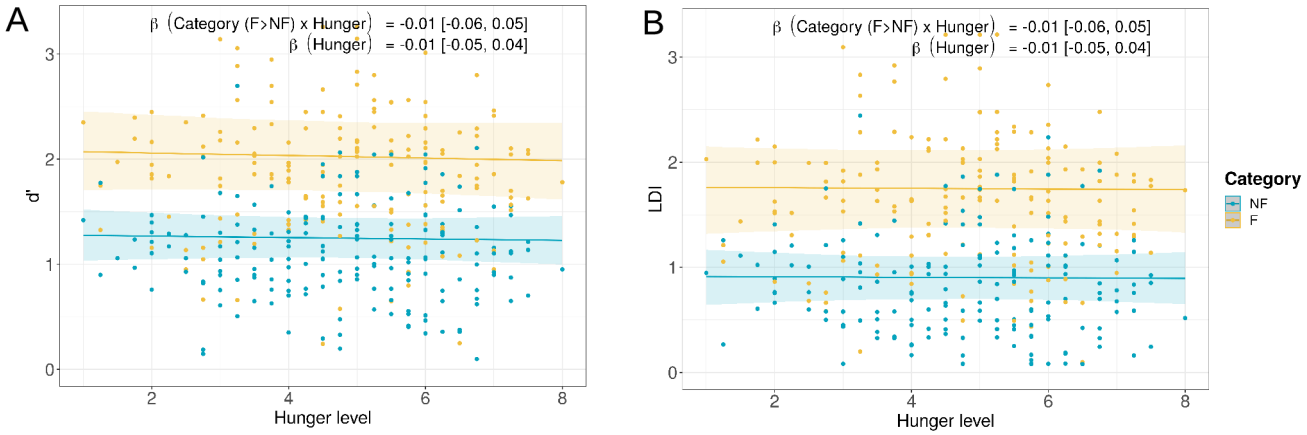

Figure 4: Memory performance depending on subjective hunger per image category. *Actual and predicted A) target recognition d' and B) lure discrimination LDI depending on subjective hunger level per image category. Points show the actual data and lines with 95%-CI depict predictions based on full model.* ***Neither d' nor LDI were affected by the subjective hunger level.*** *The estimates of the interaction of the full model (Table 1, Eq. 6, Tables 4-1 & 4-2) indicated that the image categories were not differently influenced by hunger and the estimates of the main effect of the null model (Table 1, Eq. 7, Fig. 4-1, Tables 4-1 & 4-2)) suggested that the subjective hunger level did not affect memory performance in general. Neither task-specific hunger level (Fig. 4-3) nor ghrelin serum levels as a proxy for objective hunger (Fig. 4-4, Tables 4-3 & 4-4) predicted memory performance.*

We additionally evaluated if fasted ghrelin serum levels as metabolic measure of hunger might predict target recognition or lure discrimination. However, neither food recognition nor lure discrimination performance were influenced by ghrelin levels nor did we detect an influence independent of image category (exploratory analysis, Fig. 4-4). Estimates of the predictors and random effects of all models in the model comparison are listed in the supplementary material (Tables 4-3 & 4-4).

V.3 Could the memory performance for food items (or in general) be enhanced by wanting?

Wanting defined as categories “unwanted”, “neutral” and “wanted” did neither influence recognition or lure discrimination performance in general (Fig. 5) nor food memory in specific (see non-evident interaction in Fig. 5-1). Even though the model comparison only allows for certainty regarding the lack of prediction of LDI (but not d’ due to large standard error) by wanting categories (Table 1, Eq. 9-11), the model estimates do not support a predictive effect of the wanting categories on d’ either (Fig. 5-2 & Tables 5-1 & 5-2) .

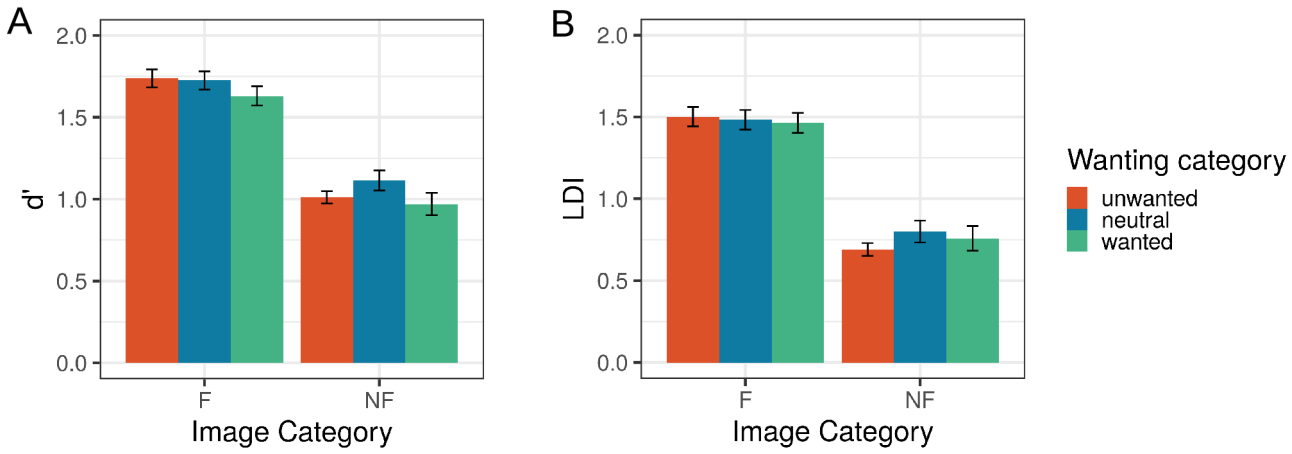

Figure 5: Memory performance depending on wanting and image category. *A) Target recognition d’ and B) lure discrimination LDI depending on wanting and image category. Depicted are mean d’ (LDI) ± standard error. Predictions by the full model are depicted in Fig. 5-1.* ***Neither d’ nor LDI were predicted by wanting category.*** *Estimates of all predictors and covariates are listed in Fig. 5-2 and Tables 5-1 & 5-2.*

V.3.a Does single item wanting influence response accuracy? (exploratory)

Wanting ratings of the single images predicted response accuracy. This evident enhancement by higher wanting is visually slightly stronger for art compared to food images (Fig. 6). Even though the

predictive accuracy of the full model (Table 1, Eq. 12) was evidently higher compared to the null models (Table 1, Eq. 13 & 14), the estimate of the interaction effect of image category and wanting does not allow for confident inferences as the credible interval of the interaction effect includes Zero (for all model estimates see Table 6-1). Therefore, we conducted post-hoc analyses in which we detected wanting enhancement for food and art separately (model estimates see Table 6-2 & Table 6-3). In sum, the wanting main effect's mean estimate (Fig. 6) as well as its odds ratio in the full model (Fig. 6-1A) and the null model without interaction (Fig. 6-1B) confirm a general enhancement of response accuracy by single item wanting.

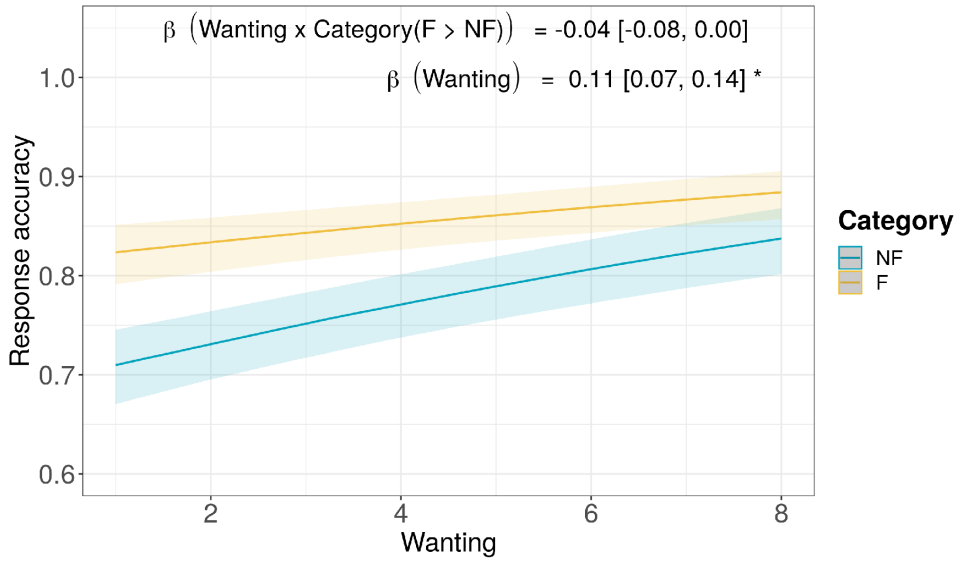

Figure 6: Predicted response accuracy by single image wanting rating per image category. *Predictions are based on full model (Table 1, Eq. 12). The estimate of the interaction suggests that the two image categories are slightly but not evidently differently influenced by the wanting rating.* ***Higher wanting enhances response accuracy*** *as the estimate of the main effect of the full model reveals but wanting might play a more important role for the art/non-food (NF) images. Odds ratios of all predictors and covariates are listed in Fig. 6-1 and Table 6-1. Odds ratios of the wanting effect per image category are listed separately in Tables 6-2 & 6-3.*

V.3.b Is the effect of single item wanting on response accuracy stronger during memory encoding? (exploratory)

The enhancement of response accuracy by higher single item wanting was strongest for the old images across food and art images, i.e. during memory encoding (Table 7-1). Response accuracy for new and similar images was not modulated by wanting. Independent of wanting, the response accuracy for new images was clearly higher than for old images and lowest for similar images (Fig. 7). Similar images were evidently worse discriminated among the art images compared to the food images (Fig. 7-1,).

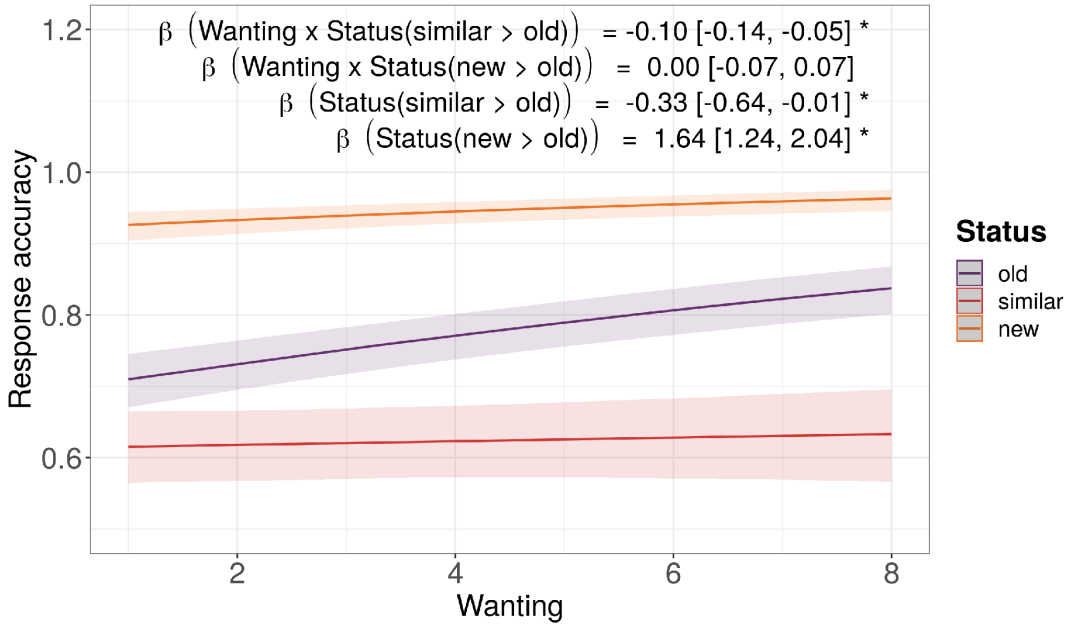

Figure 7: Predicted response accuracy by single image wanting rating for old, similar and new images respectively. *Predictions are based on full model (Table 1, Eq. 15). The estimates of the interactions endorsed the visually evident effect that* ***the wanting enhancement of the response accuracy is strongest*** *for the old images, namely* ***during memory encoding.*** *Response accuracy for new images was higher than for old images and lowest for similar images. Odds ratios of all predictors and covariates are listed in Fig. 7-1 and Table 7-1.*

V.4 Does the coherence of the entire uncinate fasciculus (UF) or a sub-bundle of the UF influence food memory performance?

We derived the tracts of the UF from deterministic tractography. The microstructural coherence of the UF reflects in the average normalized quantitative anisotropy (nQA) of the whole tract. The nQA of the entire UF was higher compared to the nQA of the sub-bundle of the UF which we traced as a proxy for a direct communication pathway from OFC to MTL (Table 3). nQA values of the UF ranged from about 0.21 to 0.33 and were comparable for both hemispheres (paired Bayesian ttest: BF = 0.09). nQA values of the sub-bundle ranged from about 0.10 to 0.26 and were evidently different between hemispheres (paired Bayesian ttest: BF = 52852.47). The magnitude of nQA values of the UF was comparable to whole brain nQA. Figure 8 displays exemplary fiber tracts of the entire UF and its sub-bundle. We tested for the role of the microstructural properties of the UF and its sub-bundle in (food) memory processes but our hypotheses were not hemisphere-specific. Therefore, we used the average nQA value of the UF and the sub-bundle of the UF per participant per session for statistical analyses. Microstructural coherence of the UF did not predict neither food nor art target recognition or lure discrimination performance (Fig. 9 A&B) nor independently of image category (Fig. 9-1 A&B). Neither did the sub-bundle of the UF predict category-specific memory performance (Fig. 9 C&D) nor independently of image category (Fig. 9-1 C&D). In both cases, the full-null model comparisons did not lead to conclusive predictive accuracies (Table 1, Eq. 19-23 and Table 2, Eq. 24-28) but the posterior distributions of the main effects of nQA emphasize a lack of a confident effect of microstructural coherence (Fig. 9-2). The interaction additionally showed that neither the UF nor its sub-bundle moderated the evident effect of image category (Fig. 9-2 & 9-3). Estimates of all models in the comparison are listed in the supplementary material (Tables 9-1 & 9-2). Due to the evident difference between left and right sub-bundles of the UF, we reran the models for left and right sub-

bundles respectively. However, these exploratory analyses did not reveal a hemisphere-specific role of the sub-bundle of the UF in memory processes (Fig. 9-4)

Table 2: Model equations of full and null models and the difference in predictive accuracy.

Eq. No.	Model Title	Model type	Model Equation dependent variable ~ predictors & covariates (without random effects for visual clarity)	Difference in Predictive Accuracy (Δelpd ± se)
24	**sub-UF**	full model	d' / LDI ~ Image Category + Wanting Category + Subj Hunger Level + nQA(sub-UF) + Image Category*nQA(sub-UF) + Wanting Category*nQA(sub-UF) + Subj Hunger Level*nQA(sub-UF) + Age + Gender + Intervention + Timepoint + Intervention*Timepoint	d' : -4.4 ± 1.6 LDI: -3.3 ± 2.1
25	**sub-UF**	null model 7	d' / LDI ~ Image Category + Wanting Category + Subj Hunger Level + nQA(sub-UF) + Age + Gender + Intervention + Timepoint + Intervention*Timepoint	d': -2.4 ± 0.5 LDI: -2.6 ± 1.0
26	**sub-UF**	null model 11	d' / LDI ~ Image Category + nQA(sub-UF) + Age + Gender + Intervention + Timepoint + Intervention*Timepoint	d': -1.9 ± 2.1 LDI: -0.2 ± 0.4
27	**sub-UF**	null model 13	d' / LDI ~ Image Category + Wanting Category + Age + Gender + Intervention + Timepoint + Intervention*Timepoint	d': reference elpd LDI: -0.8 ± 1.0
28	**sub-UF**	null model 14	d' / LDI ~ Image Category + Age + Gender + Intervention + Timepoint + Intervention*Timepoint	d': -0.6 ± 2.0 LDI: reference elpd
29	**Wanting/UF**	full model	Response accuracy ~ Image Category + Wanting + Subj Hunger Level + nQA((sub)UF) + Image Category*nQA((sub)UF) + Wanting*nQA((sub)UF) + Subj Hunger Level*nQA((sub)UF) + Age + Gender + Intervention + Timepoint + Intervention*Timepoint	response accuracy: -2.4 ± 1.1
30	**Wanting/UF**	null model 1	Response accuracy ~ Image Category + Wanting + Subj Hunger Level + nQA(UF) + Image Category*nQA(UF) + Subj Hunger Level*nQA(UF) + Age + Gender + Intervention + Timepoint + Intervention*Timepoint	response accuracy: -3.0 ± 0.5
31	**Wanting/UF**	null model 3	Response accuracy ~ Image Category + Wanting + Subj Hunger Level + nQA(UF) + Age + Gender + Intervention + Timepoint + Intervention*Timepoint	response accuracy: -1.3 ± 0.4
32	**Wanting/UF**	null model 4	Response accuracy ~ Image Category + Wanting + Subj Hunger Level + Age + Gender + Intervention + Timepoint + Intervention*Timepoint	response accuracy: evidently highest elpd
33	**Single item liking (old images)**	full model	Response accuracy ~ Image Category + Liking + Image Category*Liking + Age + Gender + Intervention + Timepoint + Intervention*Timepoint	response accuracy: -0.5 ± 0.8
34	**Single item liking (old images)**	null model 1	Response accuracy ~ Image Category + Liking + Age + Gender + Intervention + Timepoint + Intervention*Timepoint	response accuracy: reference elpd
35	**Single item liking (old images)**	null model 2	Response accuracy ~ Image Category + Age + Gender + Intervention + Timepoint + Intervention*Timepoint	response accuracy: -3.6 ± 2.5
36	**Calorie content (food images)**	full model	Response accuracy ~ Wanting + Calorie Content + Wanting*Calorie Content + Image Status + Age + Gender + Timepoint + Intervention + Timepoint*Intervention	response accuracy: -1.9 ± 2.5
37	**Calorie content (food images)**	null model 1	Response accuracy ~ Wanting + Calorie Content + Image Status + Age + Gender + Timepoint + Intervention + Timepoint*Intervention	response accuracy: -0.4 ± 2.2
38	**Calorie content (food images)**	null model 2	Response accuracy ~ Wanting + Image Status + Age + Gender + Timepoint + Intervention + Timepoint*Intervention	response accuracy: reference elpd
39	**Neuroticism**	full model	d' / LDI ~ Neuroticism + Neuroticism * Gender + Neuroticism * Age + Gender + Age	d': -0.4 ± 1.0 LDI: -0.8 ± 0.7
40	**Neuroticism**	null model 1	d' / LDI ~ Neuroticism + Neuroticism * Gender + Gender + Age	d': -0.3 ± 1.0 LDI: -0.4 ± 0.7
41	**Neuroticism**	null model 2	d' / LDI ~ Neuroticism + Gender + Age	d': reference elpd LDI: reference elpd
42	**Neuroticism**	null model 3	d' / LDI ~ Gender + Age	d': -2.0 ± 1.6 LDI: -1.1 ± 1.5
43	**Microstructural coherence**	full model	nQA(UF) ~ Gender + Age + Gender*Age + Timepoint*Intervention + Timepoint + Intervention	nQA(UF): -0.6 ± 2.9
44	**Microstructural coherence**	null model 1	nQA(UF) ~ Gender + Age + Gender*Age + Timepoint + Intervention	nQA(UF): -1.3 ± 1.8
45	**Microstructural coherence**	null model 2	nQA(UF) ~ Gender + Age + Timepoint + Intervention	nQA(UF): -2.0 ± 3.3
46	**Microstructural coherence**	null model 3	nQA(UF) ~ Gender + Timepoint + Intervention	nQA(UF): -0.5 ± 1.1
47	**Microstructural coherence**	null model 4	nQA(UF) ~ Timepoint + Intervention	nQA(UF): reference elpd

Table 3: Mean, standard deviation and range of normalized quantitative anisotropy values (nQA) of the uncinate fasciculus (UF) and its sub-bundle as well as the whole brain

nQA	left UF	right UF	average UF	left sub-bundle of UF	right sub-bundle of UF	average sub-bundle of UF	whole brain
Mean(SD)	.271 (.021)	.271 (.023)	.271 (.022)	.183 (.024)	.171 (.028)	.177 (.023)	.274 (.021)
Range	.211 - .0318	.208 - .326	.213 - .320	.111 - .243	.100 - .264	.105 - .234	.209 - .329

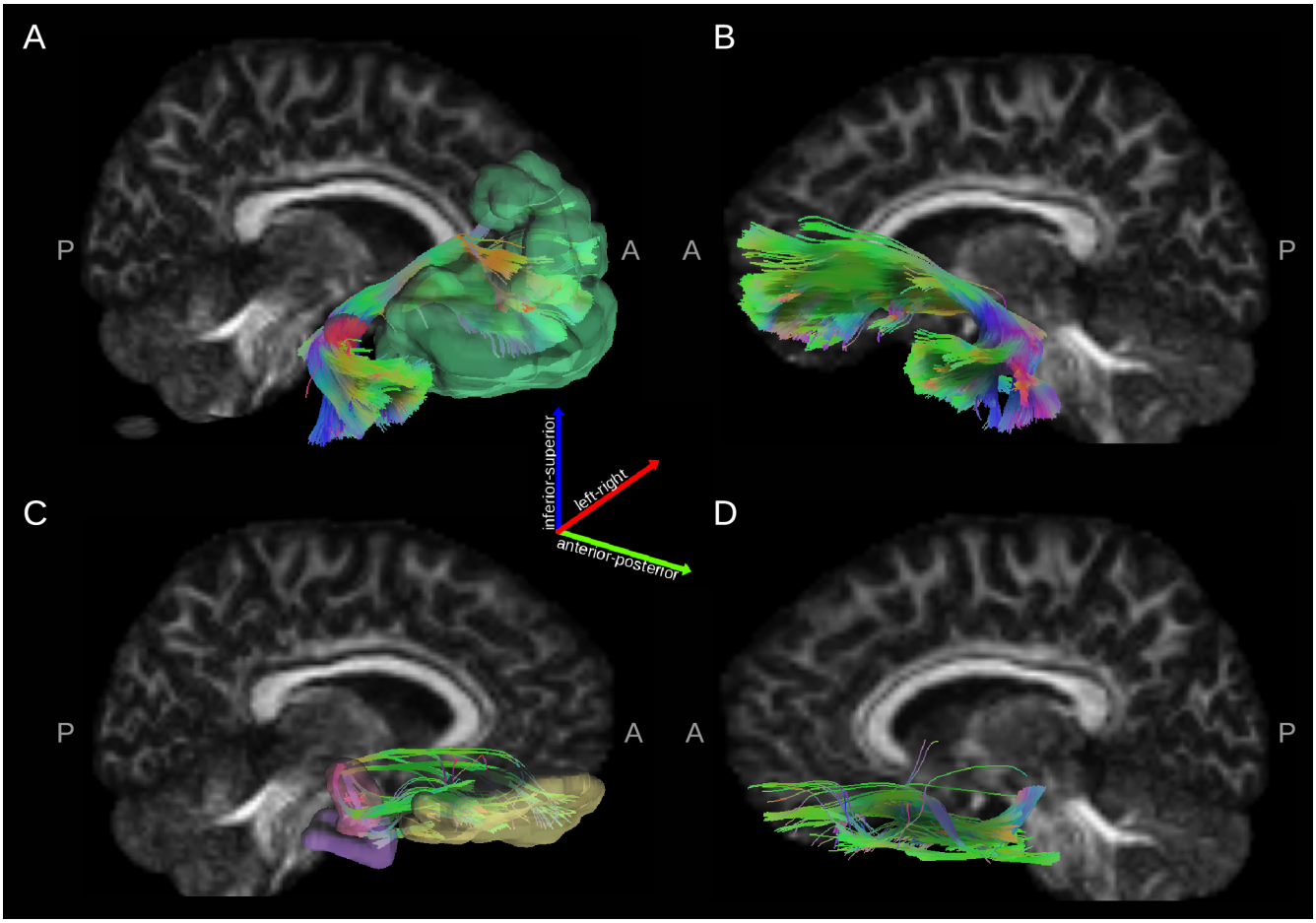

Figure 8: Exemplary tracing results of in-vivo uncinate fasciculi (UF) and sub-bundles of the UF. *A: right UF with ROIs, B: left UF, C: right sub-bundle with ROIs, D: left sub-bundle. Fiber tracts are derived from deterministic tractography conducted in DSI studio (version 2022.01.11) overlaid on a subject's whole brain normalized quantitative anisotropy map. A) Regions-of-interest for tractography of the entire UF, exemplary for the right hemisphere: red: UF seed region from John Hopkins university (JHU) labels atlas (1mm), merged end region (green) consisting of Brodman Areas 11 and 47 identical to Granger et al.(2021) and Brodman area 10 from Brodman atlas (within DSI studio). C) Regions-of-interest for tractography of sub-bundle of the UF, exemplary for the right hemisphere: yellow: seed orbitofrontal cortex regions from the AAL2 atlas (within DSI studio), pink amygdala from the FreeSurferDKT subcortical atlas and violet: the entorhinal cortex from the FreeSurferDKT cortical atlas. Orientations: A: anterior, P: posterior.*

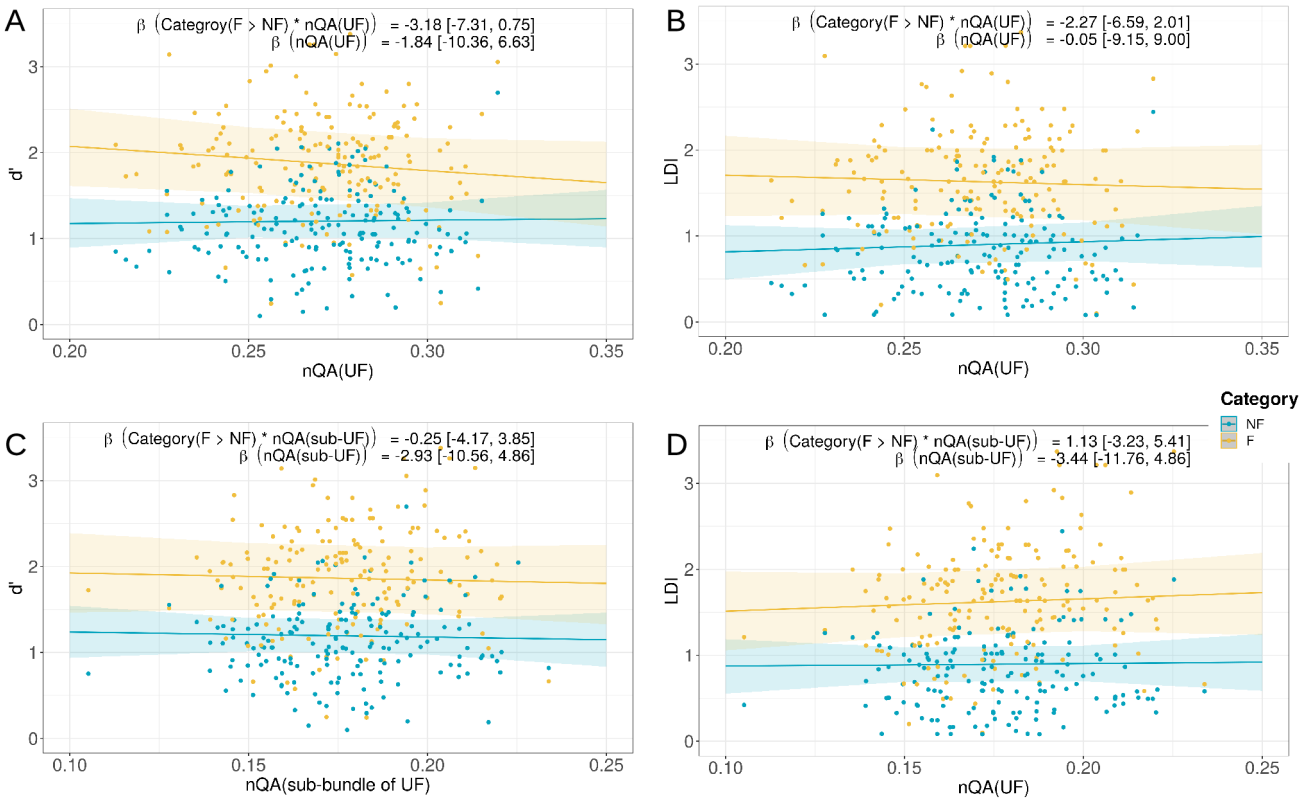

Figure 9: Memory performance depending on microstructural coherence of UF and its sub-bundle per category. *Actual and predicted A+C) target recognition d' and B+D) lure discrimination LDI depending on normalized quantitative anisotropy (nQA) of the uncinate fasciculus (UF, A&B) and its sub-bundle (C&D). Points show the actual data and lines with 95%-CI depict predictions based on full models (Table 1, Eq. 19 & Table 2, Eq. 24).* ***Neither d' nor LDI were affected by the microstructural coherence of the UF, reflected in nQA, or by its sub-bundle.*** *The estimates of the interaction of the full model indicated that the image categories were not differently influenced by the UF's microstructural coherence. The estimates of the main effect neither support an effect of microstructural coherence on memory performance (Fig. 9-1). Estimates of all predictors and covariates are visualized in Fig. 9-2 & 9-3 and listed in Tables 9-1, 9-2, 9-3 & 9-4. A hemisphere-specific role of the sub-bundle of the UF could not be confirmed (Fig. 9-4).*

V.4.a Is the compactness of the individuals white matter relevant when investigating microstructural effects? (exploratory)

In order to exclude an influence of inter-individual differences in whole brain white matter density, we re-ran all models, addressing the effect of microstructural coherence on memory performance

measures, taking whole brain nQA values into account. We corrected the nQA(UF) and nQA(sub-UF) for global white matter density. Thereto, we calculated relative nQA values by division through nQA(whole brain). We could not find an evident effect of these relative microstructural coherence measures on target recognition or lure discrimination performance – neither by relative nQA(UF) nor by relative nQA(sub-UF).

V.4.b Is the detected positive wanting effect on response accuracy moderated by the microstructural coherence of the UF? (exploratory)

We hypothesized that the UF might have a modulatory role on the interplay of wanting and memory. As the wanting categories did not evidently differ regarding memory performance measures, we extended the analysis to a possible moderation of single item wanting enhancement of response accuracy by microstructural properties of the UF. However, we did not detect a moderation neither for all images nor for old images, for which the wanting enhancement was most pronounced. The mean estimates (Fig. 10) and median odds ratios (Fig. 10-1) of the posterior distributions of the nQA(UF)*wanting interaction supported this lack of modulatory top-down control. Odds ratios of the predictors and random effects of all models in the model comparison are listed in Table 10-1. In summary, the positive wanting effect on response accuracy was not evidently moderated by the microstructural coherence of the UF.

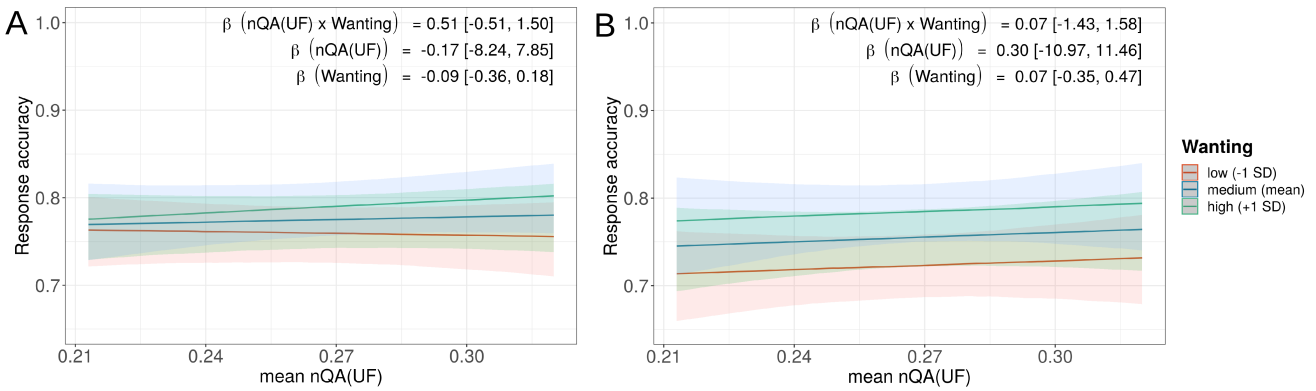

Figure 10: Predicted response accuracy by wanting depending on the microstructural integrity of the UF. *Predictions are based on the full model (Table 2, Eq. 29) A) for all images and B) for old images only. The estimates of the interactions endorsed the visually evident lack of a moderation effect of nQA(UF) on the wanting enhancement of the response accuracy. Odds ratios of all predictors and covariates are visualized in Fig. 10-1 and listed in Table 10-1.*

V.5 Further behavioural analyses

In order to discuss the enhanced response accuracy by wanting during memory encoding, we additionally considered the effects of general preference (i.e. liking). The enhancement by wanting compared to liking during memory encoding is slightly stronger which is supported by the slight difference in mean estimates of the main effects (Fig. 11 A & B). The estimate of the interaction of liking with image category suggested that enhancement during memory encoding by liking is similar for food and art images (Fig 11 A, Table 11-1). The same can be concluded for the enhancement by wanting (Fig 11 B, Table 11-2). Even though the model comparison (Table 2, Eq. 33-35) did not allow for a confident exclusion of the liking-image category interaction effect, the comparison supported the enhanced response accuracy through liking.

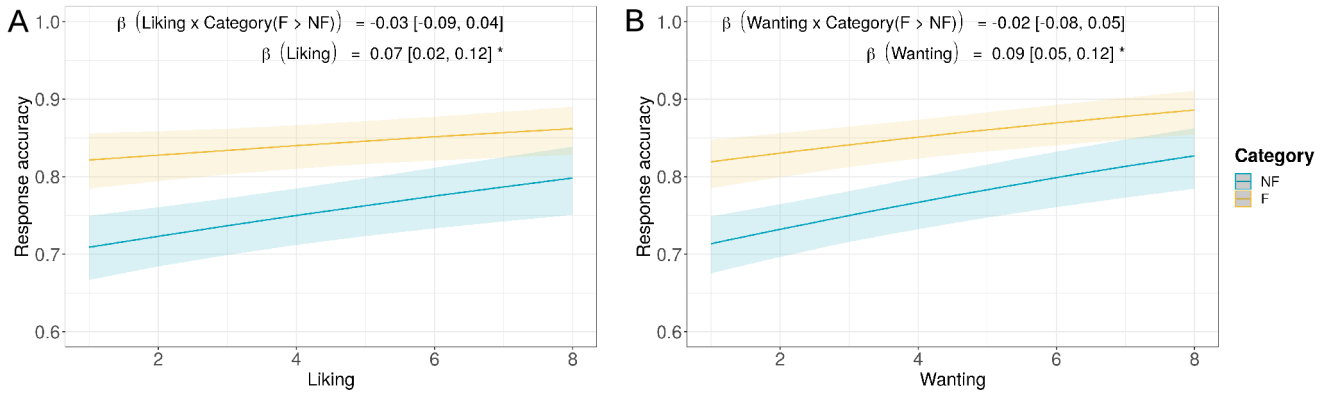

Figure 11: Recognition accuracy of old images predicted by A) liking and B) wanting. *Depicted are predictions and their 95%-CI based on full model (Table 2, Eq. 33). The estimates of the interaction of the full model indicate that wanting and liking affect both image categories similarly. The enhancement by wanting during memory encoding is slightly stronger than by general liking. Odds ratios of the corresponding models are listed in Tables 11-1 & 11-2.*

As preregistered, we investigated if body composition measures, namely BMI, gender-standardized waist-to-hip ratio and gender-standardized fat mass, affect food memory performance. Neither target recognition nor lure discrimination were predicted by body composition measures nor did we find differences between food and art memory performance. We investigated if possible effects of nausea, anxiety, difficulty of the tasks or exhaustion by the tasks affected memory performance. None of these well-being measures influenced the participants' performance on the memory task (see GitLab repository).

Calorie content did not influence response accuracy of the food images evidently. Neither the model comparison (Table 2, Eq. 36-38) nor the estimates of the main effects (Fig. 12, Fig. 12-1 A) did allow for confident inference about the role of calorie content for food memory accuracy. The wanting enhancement of response accuracy did not depend on calorie content of the depicted food (Table 2, Eq. 36, Fig. 12-1B, Table 12-1).

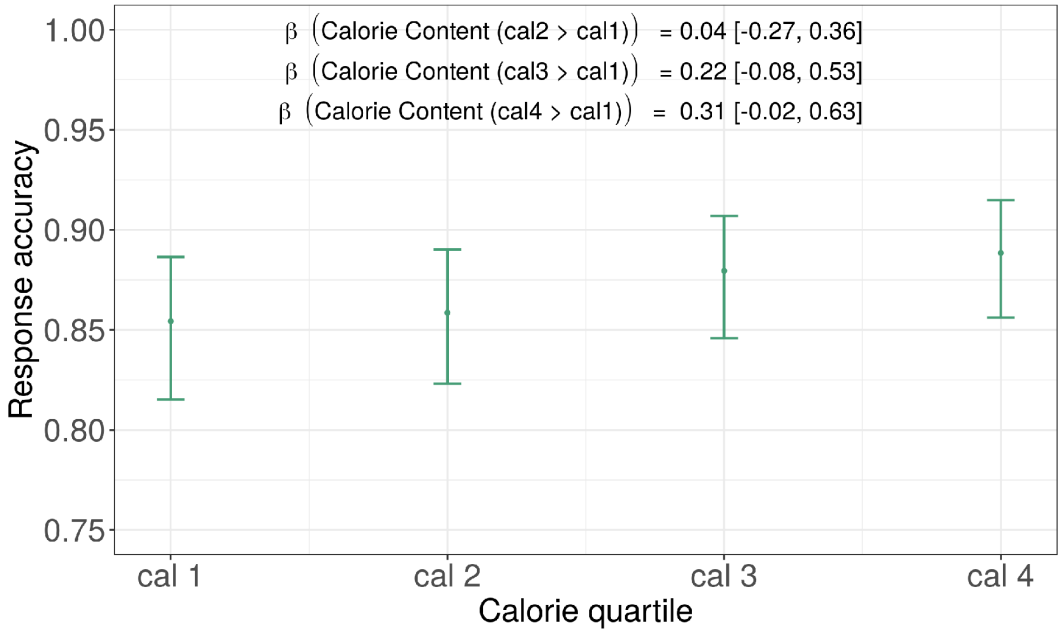

Figure 12: Response accuracy predicted by calorie content of the food items. *Predictions are based on the null model 1 (Table 2, Eq. 37). Mean predictions and their 95%-CI are depicted. Calorie content does not evidently influence response accuracy of the food images. Odds ratios of all predictors and covariates are visualized in Fig. 12-1 and listed in Table 12-1.*

Female participants (n=20) outperformed male participants (n=40) in the memory task. Target recognition, lure discrimination and memory accuracy were predicted by gender which was included as covariate in all Bayesian regression models (see Fig. 13). With additional exploratory analyses, we aimed to understand this gender difference. The analyses included interactions of gender with socio-economic status, attention network performance, personality traits and eating behaviour traits, as well as their main effects. Gender interaction effects on target recognition or lure discrimination performance could not be confirmed. However, the personality trait "neuroticism" predicted target recognition and lure discrimination performance. We found that the more neurotic the participants the worse their memory performance (Fig. 14). This effect was independent of their gender and age

(Tables 14-1 & 14-2).

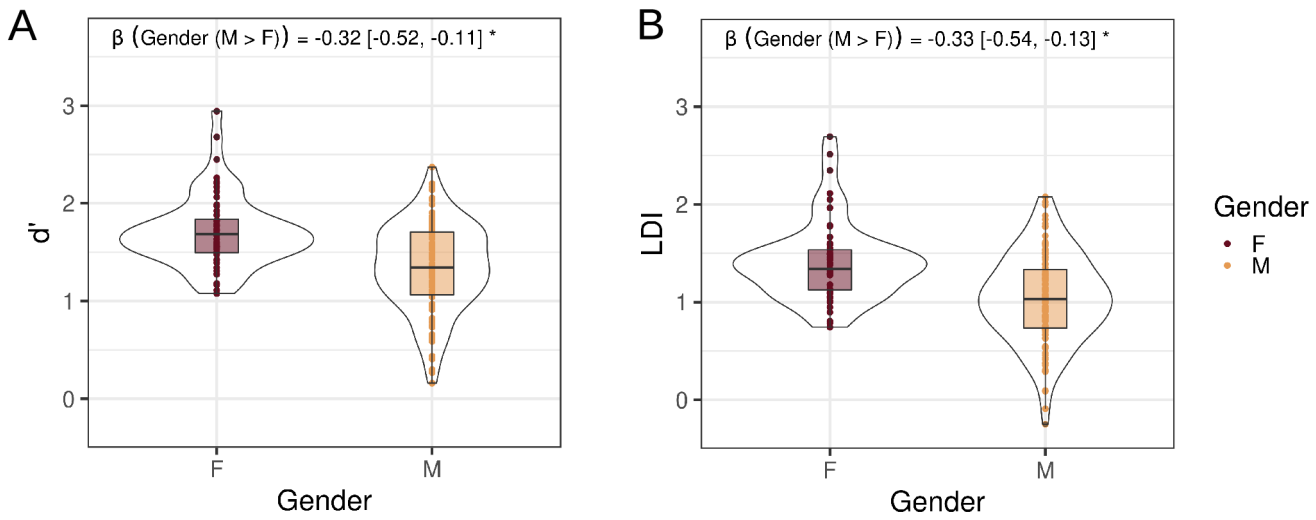

Figure 13: Memory performance per gender group. *A) The* ***target recognition d' and B) the lure discrimination LDI of female (F) participants*** *(bordeaux)* ***is better than of male participants (M)*** *(orange). Violin plots present the distribution of the two indices per gender. The estimate's CI did not include 0 which indicated an evident difference in memory performance between gender groups.*

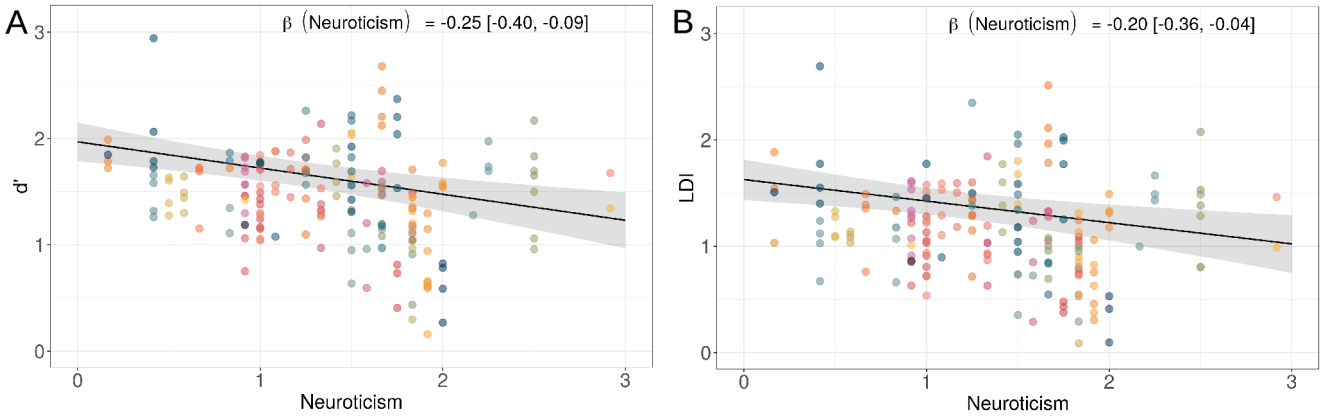

Figure 14: Memory performance depending on personality trait neuroticism. *Actual and predicted A) target recognition d' and B) lure discrimination LDI depending on neuroticism assessed with the NEO-FFI. Points show the actual data and lines with 95%-CI depict predictions based on null model 2 (Table 2, Eq. 41). d' and LDI were evidently predicted by neuroticism.* ***The more neurotic the participants, the worse their memory performance.*** *Estimates of the corresponding models are listed in Tables 14-1 & 14-2.*

V.6 Further DWI analyses

Microstructural coherence of the UF was neither decreased by age (Fig. 15 A) nor evidently different between females and males (Fig. 15 B). The model comparison (Table 2, Eq. 43-47) did not allow for confident inferences about possible effects on UF microstructure. Nevertheless, the model estimates indicated a lack of an age and/or gender effect (see Table 15-1). An impact of the individuals' body composition reflected in BMI, WHR (gender-standardized) and FM (gender-standardized) was equally undetectable. In summary, neither the microstructural coherence of the UF nor of the whole brain (Fig. 15-1) was affected by gender, age or body composition.

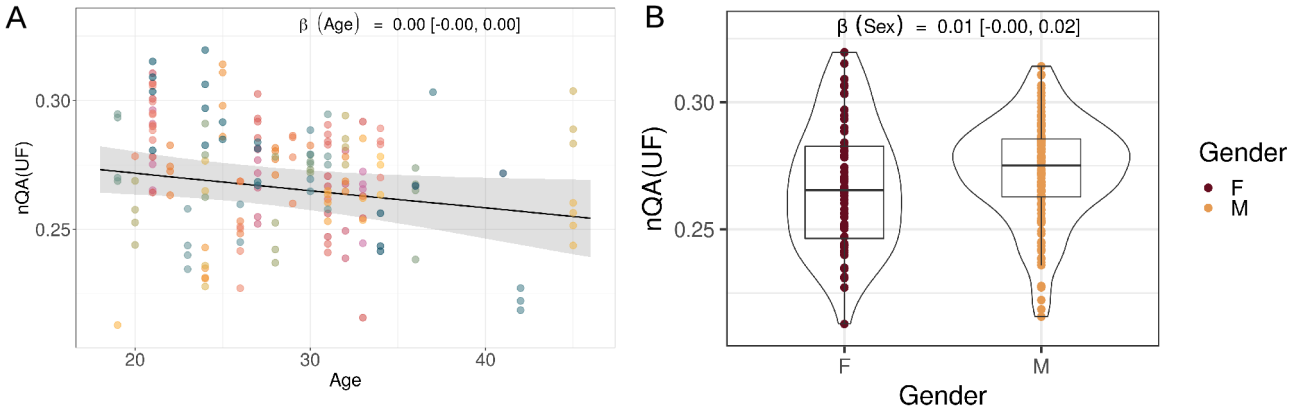

Figure 15: Microstructural coherence of UF depending on age and gender. *Actual and predicted microstructural coherence of the UF, reflected in its nQA value, A) by age and B) by gender. Points show actual data of the color-coded subjects. A) Prediction line with 95%-CI is based on null model 2 (Table 2, Eq. 45). B) Violin and boxplots present the distribution of the nQA values over both genders.* ***Neither age nor gender predicted the microstructural coherence of the UF.*** *Odds ratios of the corresponding models are listed in Tables 15-1. The effects of age and gender on the whole brain's microstructural coherence is shown in Fig. 15-1.*

VI Discussion

In this preregistered study combining in-depth behavioural, physiological and advanced neuroimaging data from 60 adults (20 females) of up to 4 time points, we find that desire to eat (i.e. food wanting) predicted recognition of food items, and that food was better memorized than art images. In contrast, we could not detect a moderating effect of microstructural measures of the uncinate fasciculus on memory performance, extracted from diffusion imaging, in this homogeneous cohort of 20 to 41 year old adults. Exploratory results indicated effects of gender and personality traits on memory performance.

Food images were better recognized and discriminated than art images. Evolutionary seen, the ability to recognize and discriminate visual details of food items has been important to differentiate between edible and potentially toxic food items, e.g. berries or mushrooms. This bias of greater attention to food stimuli(Kumar et al., 2016) might explain increased recognition and discrimination performance(Humphreys et al., 2010). In our study, we confirmed that food is better recognized and discriminated than art images. Nevertheless, complexity of the art images was higher which could partly explain their lower recognition and discrimination. However, the influence of image complexity is highly individual(Marin and Leder, 2013) and still controversial(Chai et al., 2010; Nguyen and McDaniel, 2015; Gomez et al., 2020). Therefore, the higher evolutionary and hedonic relevance of food compared to art might be determining food memory performance.

Subjective hunger level varied largely but did not predict memory performance in our population. Several previous studies(Morris and Dolan, 2001; Talmi et al., 2013; Montagrin et al., 2021) found an enhancing effect of hunger on food memory performance when hunger was contrasted to satiety. In our study though, participants received a standardized breakfast-shake. Thus, the difference in

perceived hunger states might not have been large enough to explain variance in food memory performance. Additionally, fasted ghrelin serum levels, as a proxy for “physiological hunger”, neither predicted subsequent memory performance. However, ghrelin serum levels were not measured immediately before the task which may explain a lack of correlation with food memory compared to previous studies(Carlini et al., 2010).

The stronger the wanting to eat a certain food during memory encoding the better was the food recognition accuracy in the subsequent task in our study. This finding suggests that not only *wanting* alone determines if a certain food is chosen to eat but that food choices might also be influenced by recognition memory which is reinforced by previous rewarding experiences. Hereby, we add on previous studies showing that food choices were influenced by memories of past experiences(Higgs, 2016). Outside of the experimental context, food wanting is constantly manipulated by an overload of food stimuli in our environment. This often repetitious exposure to food stimuli might enhance the desire to eat especially high-caloric food(Duraisingam et al., 2021) as well as its recognition(Stang, 1975). On top of that manipulation, the displayed food items often have a high energy density(Powell et al., 2007) and might therefore fortify overnutrition by their over-representation in the environment. Recently, de Vries and colleagues(2022) have shown that humans’ spatial recognition memory is biased towards high-caloric compared to low-caloric food items independent of desire to eat. However meaningful for our ancestors, this calorie bias in recognition memory in combination with an increased desire to eat high-caloric food which in turn enhances recognition might be nowadays detrimental for a healthy, intuitive food decision-making. In our study, this calorie bias in recognition memory accuracy was not evident, possibly due to the grouping into calorie quartiles. Besides the enhancement of food recognition accuracy through food wanting, this wanting enhancement could also be detected for the art images. Hence, recognition of single items in general seems to be fortified through desire.

Considering the close link of reward and emotion(Baxter et al., 2000; Murray, 2007) and previous studies showing effects of emotion on target recognition d' and lure discrimination LDI(Kensinger et al., 2006; Leal et al., 2014; Szőllősi and Racsmány, 2020), we hypothesized an effect of wanting on these memory indices. However, we could not confirm this effect, possibly due to power reduction after categorizing into "unwanted", "neutral" and "wanted" images. We suppose that individualized picture sets of more intensely desired or despised food images could elicit food wanting effects on different memory sub-processes.

As wanting is distinct to liking(Berridge et al., 2009), we compared the effect of wanting during memory encoding to the participants' general liking of these encoded images. The enhancement by liking was also evident but weaker than by wanting. This finding confirms the previously claimed enhanced recognition accuracy by preference(Brooks and Watkins, 1989; Wang and Chang, 2004; Newell and Shanks, 2007) and furthers the field by adding a slightly stronger memory enhancement through wanting. Unclear is though, if liking and wanting determine recognition accuracy or if recognition enhances liking and wanting through the mere exposure effect. The direction of this relation has been previously questioned(Brooks and Watkins, 1989; Wang and Chang, 2004). In the case of a "cross-talk" between wanting and memory, the danger of a vicious cycle regarding food-decision making could arise. While speculative, this vicious cycle could consist of food choices of high-caloric, highly wanted food items and an increased recognition memory of these, which then in turn leads to a more frequent choice of these food items due to the remembered desire and positive experience.

In our study, we could not find an association between food recognition or lure discrimination performance and participants' eating behaviour. This result endorsed our screening attempt that the participants scored low on food restrictions and eating restraint. Therefore, populations with aberrant

eating traits may behave differently. Previous studies showed that restrained eaters present more extreme cravings than unrestrained eaters(Fedoroff et al., 2003). Besides higher cravings, higher calorie content has been shown to enhance spatial memory of food items and memory of eating(Seitz et al., 2021a). Therefore, studying the influence of food wanting and calorie content on food memory in restrained eaters might be insightful regarding their food decision-making.

On the neuronal level, we hypothesized a putative top-down modulatory control by microstructural properties of the uncinate fasciculus (UF) in memory processes which integrate food wanting and hunger. The UF connects brain areas which process wanting(Lebreton et al., 2009), hunger(Morris and Dolan, 2001), emotion(Gao et al., 2021) and memory(Bakker et al., 2008; Yassa and Stark, 2011) and has been previously shown to play a role in emotional memory processes(Yau et al., 2009; Granger et al., 2021). However, we could not transfer and confirm this role in wanting enhanced memory, neither for the UF nor for a sub-bundle of the UF. This sub-bundle terminates in the MTL and might carry relevant information for wanting enhanced recognition. Even though evidence is weak(Canli et al., 2000; Dolcos et al., 2004), we tested if only left hemispheric OFC-MTL communication might be relevant for wanting enhanced recognition nut could not confirm hemisphere-specific influence of the UF's sub-bundle. Another possible explanation for the lack of microstructural modulation might be that in this relatively young and healthy study population, white matter properties might not (yet) be relevant in the interaction of cognitive functions. Previous studies showed that variations or changes in white matter microstructure correlate with memory performance, but these correlations concern mainly elderly populations(Cremers et al., 2016) and populations with neuropsychological disorders(Alves et al., 2018; Subramaniam et al., 2018).

Female participants in our study outperformed male participants regarding target recognition, lure discrimination and memory accuracy but none of the assessed anthropometric, cognitive or personality

measures could explain this gender difference. However, we detected a negative influence of neuroticism on memory indices. Higher cognitive load due to neurotic behaviour might lead to reduced memory capacities. This assumption is supported by associations of neuroticism with reduced retrospective memory(Buchanan, 2017) and working memory performance(Studer-Luethi et al., 2012). Our gender-unbalanced study design does not allow for definite conclusions but in line with previous studies(Levy et al., 2005; Wang, 2013), gender differences in memory performance might be evident. Overall, through conscientious definition of our study population, advanced tractography of white matter and conservative Bayesian regression modeling(Gelman and Tuerlinckx, 2000), we are confident presented results are reliable and that the detected effects are not false positives.

In conclusion, we showed that food recognition memory is influenced by food desires. In contrast, the microstructure of implicated neural pathways, namely the UF, was not of importance for memory performance in this sample of healthy, overweight adults. Other factors unrelated to white matter connectivity could be be of higher importance for memory performance. It cannot be excluded that in populations with deteriorated white matter such as in elderly(Westlye et al., 2010) or obese(Zhang et al., 2018), the microstructural coherence of the UF might actually determine cognitive functions related to food memory. Regarding the overnutrition pandemic, cognitive behavioural therapies could be improved by strategies that connect food desires and subsequent food recognition. The interlacing of food desires and food memory could also be considered in the development of public health campaigns and regulations.

VII References

Alves GS, Knöchel C, Paulitsch MA, Reinke B, Carvalho AF, Feddern R, Prvulovic D, Sudo FK, Pantel J, Reif A, Oertel V (2018) White Matter Microstructural Changes and Episodic Memory Disturbances in Late-Onset Bipolar Disorder. Front Psychiatry 9 Available at: https://www.frontiersin.org/article/10.3389/fpsyt.2018.00480/full.

Bakker A, Brock Kirwan C, Miller M, Stark CEL (2008) Pattern Separation in the Human Hippocampal CA3 and Dentate Gyrus. Science (80-) 319:1640–1642 Available at: http://www.ncbi.nlm.nih.gov/pubmed/17303747 [Accessed July 25, 2018].

Baxter MG, Parker A, Lindner CCC, Izquierdo AD, Murray EA (2000) Control of response selection by reinforcer value requires interaction of amygdala and orbital prefrontal cortex. J Neurosci 20:4311–4319.

Berridge KC, Kringelbach ML (2008) Affective neuroscience of pleasure: Reward in humans and animals. Psychopharmacology (Berl) 199:457–480.

Berridge KC, Robinson TE, Aldridge JW (2009) Dissecting components of reward: 'liking', 'wanting', and learning. Curr Opin Pharmacol 9:65–73 Available at: https://www.sciencedirect.com/science/article/pii/S1471489208002129 [Accessed October 11, 2018].

Berthoud HR (2007) Interactions between the "cognitive" and "metabolic" brain in the control of food intake. Physiol Behav 91:486–498.

Berthoud HR (2012) The neurobiology of food intake in an obesogenic environment. Proc Nutr Soc 71:478–487.

Blechert J, Meule A, Busch NA, Ohla K (2014) Food-pics: an image database for experimental research on eating and appetite. Front Psychol 5:617 Available at: http://www.ncbi.nlm.nih.gov/pubmed/25009514 [Accessed July 31, 2018].

Borkenau P, Ostendorf F (2008) NEO-Fünf-Faktoren-Inventar nach Costa und McCrae, 2nd ed. Göttingen: Hogrefe, Verlag f. Psychologie.

Brooks JO, Watkins MJ (1989) Recognition Memory and the Mere Exposure Effect. J Exp Psychol Learn Mem Cogn 15:968–976.

Buchanan T (2017) Self-assessments of memory correlate with neuroticism and conscientiousness, not memory span performance. Pers Individ Dif 105:19–23.

Canli T, Zhao Z, Brewer J, Gabrieli JD, Cahill L (2000) Event-related activation in the human amygdala associates with later memory for individual emotional experience. J Neurosci 20:1–5.

Carlini VP, Ghersi M, Schiöth HB, de Barioglio SR (2010) Ghrelin and memory: Differential effects on acquisition and retrieval. Peptides 31:1190–1193.

Chai XJ, Ofen N, Jacobs LF, Gabrieli JDE (2010) Scene complexity: Influence on perception, memory, and evelopment in the medial temporal lobe. Front Hum Neurosci 4:1–10.

Chainay H, Michael GA, Vert-Pré M, Landré L, Plasson A (2012) Emotional enhancement of immediate memory: Positive pictorial stimuli are better recognized than neutral or negative pictorial stimuli. Adv Cogn Psychol 8:255–266.

Cremers LGM, de Groot M, Hofman A, Krestin GP, van der Lugt A, Niessen WJ, Vernooij MW, Ikram MA (2016) Altered tract-specific white matter microstructure is related to poorer cognitive performance: The Rotterdam Study. Neurobiol Aging 39:108–117 Available at: http://dx.doi.org/10.1016/j.neurobiolaging.2015.11.021.

de Vries R, Boesveldt S, de Vet E (2022) Human spatial memory is biased towards high-calorie foods: a cross-cultural online experiment. Int J Behav Nutr Phys Act 19:1–13 Available at: https://doi.org/10.1186/s12966-022-01252-w.

de Vries R, Morquecho-Campos P, de Vet E, de Rijk M, Postma E, de Graaf K, Engel B, Boesveldt S (2020) Human spatial memory implicitly prioritizes high-calorie foods. Sci Rep 10:1–6 Available at: https://doi.org/10.1038/s41598-020-72570-x.

Dolcos F, LaBar KS, Cabeza R (2004) Interaction between the amygdala and the medial temporal lobe memory system predicts better memory for emotional events. Neuron 42:855–863.

Duraisingam A, Palaniappan R, Soria D (2021) Attentional bias towards high and low caloric food on repeated visual food stimuli: An ERP study. Proc Annu Int Conf IEEE Eng Med Biol Soc EMBS:740–743.

Fan J, McCandliss BD, Sommer T, Raz A, Posner MI (2002) Testing the efficiency and independence of attentional networks. Journal of Cognitive Neuroscience. J Cogn Neurosci 14:340–347.

Fedoroff I, Polivy J, Herman CP (2003) The specificity of restrained versus unrestrained eaters' responses to food cues: General desire to eat, or craving for the cued food? Appetite 41:7–13.

Gao W, Biswal B, Chen SD, Wu XR, Yuan JJ (2021) Functional coupling of the orbitofrontal cortex and the basolateral amygdala mediates the association between spontaneous reappraisal and emotional response. Neuroimage 232:117918.

García-García I, Morys F, Michaud A, Dagher A (2020) Food Addiction, Skating on Thin Ice: a Critical Overview of Neuroimaging Findings. Curr Addict Reports 7:20–29.

Gelman A, Tuerlinckx F (2000) Type S error rates classical and Bayesian single and multiple compparison procedures. Comput Stat 15:373–390.

Gomez P, von Gunten A, Danuser B (2020) Recognizing images: The role of motivational significance, complexity, social content, age, and gender. Scand J Psychol 61:183–194.

Gottfried JA, O'Doherty J, Dolan RJ (2003) Encoding Predictive Reward Value in Human Amygdala and Orbitofrontal Cortex. Science (80-) 301:1104–1107 Available at: https://www.science.org/doi/10.1126/science.1087919.

Granger SJ, Leal SL, Larson MS, Janecek JT, McMillan L, Stern H, Yassa MA (2021) Integrity of the uncinate fasciculus is associated with emotional pattern separation-related fMRI signals in the hippocampal dentate and CA3. Neurobiol Learn Mem 177:107359.

Harris JA, Benedict FG (1918) A biometric study of human basal metabolism. Proc Natl Acad Sci U S A 4:370.

Higgs S (2016) Cognitive processing of food rewards. Appetite 104:10–17 Available at: http://dx.doi.org/10.1016/j.appet.2015.10.003.

Higgs S, Spetter MS (2018) Cognitive Control of Eating: the Role of Memory in Appetite and Weight Gain. Curr Obes Rep 7:50–59 Available at: http://www.ncbi.nlm.nih.gov/pubmed/29430616 [Accessed July 25, 2019].

Hilbert A, Tuschen-Caffier B, Karwautz A, Niederhofer H, Munsch S (2007) Eating Disorder Examination-Questionnaire. Diagnostica 53:144–154 Available at: https://econtent.hogrefe.com/doi/10.1026/0012-1924.53.3.144.

Humphreys L, Underwood G, Chapman P (2010) Enhanced memory for emotional pictures: A product of increased attention to affective stimuli? Eur J Cogn Psychol 22:1235–1247 Available at: http://www.tandfonline.com/doi/abs/10.1080/09541440903427487 [Accessed June 2, 2022].

Kensinger EA (2007) Negative Emotion Enhances Memory Accuracy. Curr Dir Psychol Sci 16:213–218.

Kensinger EA, Garoff-Eaton RJ, Schacter DL (2006) Memory for specific visual details can be enhanced by negative arousing content. J Mem Lang 54:99–112.

Kensinger EA, Schacter DL (2006) Amygdala activity is associated with the successful encoding of item, but not source, information for positive and negative stimuli. J Neurosci 26:2564–2570.

Kumar S, Higgs S, Rutters F, Humphreys GW (2016) Biased towards food: Electrophysiological evidence for biased attention to food stimuli. Brain Cogn 110:85–93 Available at: http://dx.doi.org/10.1016/j.bandc.2016.04.007.

Lampert T, Kroll LE, Müters S, Stolzenberg H (2013) Messung des sozioökonomischen Status in der Studie „Gesundheit in Deutschland aktuell" (GEDA). Bundesgesundheitsblatt - Gesundheitsforsch - Gesundheitsschutz 56:131–143 Available at: http://link.springer.com/10.1007/s00103-012-1583-3.

Leal SL, Tighe SK, Yassa MA (2014) Asymmetric effects of emotion on mnemonic interference. Neurobiol Learn Mem 111:41–48 Available at: http://dx.doi.org/10.1016/j.nlm.2014.02.013.

Lebreton M, Jorge S, Michel V, Thirion B, Pessiglione M (2009) An Automatic Valuation System in the Human Brain: Evidence from Functional Neuroimaging. Neuron 64:431–439 Available at: https://www-sciencedirect-com.browser.cbs.mpg.de/science/article/pii/S089662730900751X [Accessed October 22, 2018].

Levy LJ, Astur RS, Frick KM (2005) Men and women differ in object memory but not performance of a virtual radial maze. Behav Neurosci 119:853–862 Available at: /record/2005-11024-001 [Accessed June 7, 2022].

Marin MM, Leder H (2013) Examining Complexity across Domains: Relating Subjective and Objective Measures of Affective Environmental Scenes, Paintings and Music Patterson RL, ed. PLoS One 8:e72412 Available at: https://dx.plos.org/10.1371/journal.pone.0072412.

Medawar E, Thieleking R, Witte AV (2022) Dietary Fiber and WHO Food Categories Extension for the Food-Pics_Extended Database. Front Psychol 13:1–5.

Montagrin A, Martins-Klein B, Sander D, Mather M (2021) Effects of hunger on emotional arousal responses and attention/memory biases. Emotion 21:148–158 Available at: http://doi.apa.org/getdoi.cfm?doi=10.1037/emo0000680.

Morris JS, Dolan RJ (2001) Involvement of Human Amygdala and Orbitofrontal Cortex in Hunger-Enhanced Memory for Food Stimuli. J Neurosci 21:5304–5310.

Murray EA (2007) The amygdala, reward and emotion. Trends Cogn Sci 11:489–497.

Newell BR, Shanks DR (2007) Recognising what you like: Examining the relation between the mere-exposure effect and recognition. Eur J Cogn Psychol 19:103–118.

Nguyen K, McDaniel MA (2015) The picture complexity effect: Another list composition paradox. J Exp Psychol Learn Mem Cogn 41:1026–1037.

Pisner DA, Smith R, Alkozei A, Klimova A, Killgore WDS (2017) Highways of the emotional intellect: white matter microstructural correlates of an ability-based measure of emotional intelligence. Soc Neurosci 12:253–267 Available at: https://www.tandfonline.com/doi/full/10.1080/17470919.2016.1176600.

Powell LM, Szczypka G, Chaloupka FJ (2007) Adolescent Exposure to Food Advertising on Television. Am J Prev Med 33:251–256.

Pudel V, Westenhöfer J (1989) Fragebogen zum Eßverhalten (FEV)-Handanweisung. Göttingen: Hogrefe, Verlag f. Psychologie.

R Core Team . (2021) R: A Language and Environment for Statistical Computing. Available at:

https://www.r-project.org/.

Richardson MP, Strange BA, Dolan RJ (2004) Encoding of emotional memories depends on amygdala and hippocampus and their interactions. Nat Neurosci 7:278–285 Available at: http://www.nature.com/articles/nn1190 [Accessed July 6, 2018].

Roesler R, McGaugh JL (2022) The Entorhinal Cortex as a Gateway for Amygdala Influences on Memory Consolidation. Neuroscience.

Rozin P, Zellner D (1985) The Role of Pavlovian Conditioning in the Acquisition of Food Likes and Dislikes. Ann N Y Acad Sci 443:189–202 Available at: /record/1986-14517-001 [Accessed June 2, 2022].

Seitz BM, Blaisdell AP, Tomiyama AJ (2021a) Calories count: Memory of eating is evolutionarily special. J Mem Lang 117:104192 Available at: https://linkinghub.elsevier.com/retrieve/pii/S0749596X20301066.

Seitz BM, Tomiyama AJ, Blaisdell AP (2021b) Eating behavior as a new frontier in memory research. Neurosci Biobehav Rev 127:795–807.

Spetter MS, Higgs S, Dolmans D, Thomas JM, Reniers RLEP, Rotshtein P, Rutters F (2020) Neural correlates of top-down guidance of attention to food: An fMRI study. Physiol Behav 225:113085 Available at: https://doi.org/10.1016/j.physbeh.2020.113085.

Stang DJ (1975) Effects of “mere exposure” on learning and affect. J Pers Soc Psychol 31:7–12.

Stevenson RJ, Francis HM (2017) The hippocampus and the regulation of human food intake. Psychol Bull 143:1011–1032.

Studer-Luethi B, Jaeggi SM, Buschkuehl M, Perrig WJ (2012) Influence of neuroticism and conscientiousness on working memory training outcome. Pers Individ Dif 53:44–49.

Subramaniam K, Gill J, Fisher M, Mukherjee P, Nagarajan S, Vinogradov S (2018) White matter microstructure predicts cognitive training-induced improvements in attention and executive functioning in schizophrenia. Schizophr Res 193:276–283 Available at: https://linkinghub.elsevier.com/retrieve/pii/S0920996417304012.

Szőllősi Á, Racsmány M (2020) Enhanced mnemonic discrimination for emotional memories: the role of arousal in interference resolution. Mem Cogn 48:1032–1045.

Talmi D, Ziegler M, Hawksworth J, Lalani S, Herman CP, Moscovitch M (2013) Emotional stimuli exert parallel effects on attention and memory. Cogn Emot 27:530–538.

Thiebaut de Schotten M, Dell’Acqua F, Valabregue R, Catani M (2012) Monkey to human comparative anatomy of the frontal lobe association tracts. Cortex 48:82–96 Available at: http://dx.doi.org/10.1016/j.cortex.2011.10.001.

Thieleking R, Medawar E, Disch L, Witte AV (2020) art.pics Database: An Open Access Database for Art Stimuli for Experimental Research. Front Psychol 11:1–15.

Thieleking R, Zhang R, Paerisch M, Wirkner K, Anwander A, Beyer F (2021) Same brain , different look ? The impact of scanner, sequence and preprocessing on diffusion imaging outcome parameters. :1–28.

van Doorn J, Aust F, Haaf JM, Stefan AM, Wagenmakers EJ (2021) Bayes Factors for Mixed Models. Comput Brain Behav.

Vehtari A, Gelman A, Gabry J (2017) Practical Bayesian model evaluation using leave-one-out cross-validation and WAIC. Stat Comput 27:1413–1432 Available at: http://link.springer.com/10.1007/s11222-016-9696-4.

Von Der Heide RJ, Skipper LM, Klobusicky E, Olson IR (2013) Dissecting the uncinate fasciculus: Disorders, controversies and a hypothesis. Brain 136:1692–1707.

Wang MY, Chang HC (2004) The mere exposure effect and recognition memory. Cogn Emot 18:1055–1078.

Wang Q (2013) Gender and emotion in everyday event memory. Memory 21:503–511 Available at: https://www.tandfonline.com/doi/abs/10.1080/09658211.2012.743568 [Accessed June 7, 2022].

Warlow SM, Berridge KC (2021) Incentive motivation: ‘wanting’ roles of central amygdala circuitry. Behav Brain Res 411:113376.

Westlye LT, Walhovd KB, Dale AM, Bjørnerud A, Due-Tønnessen P, Engvig A, Grydeland H, Tamnes CK, Østby Y, Fjell AM (2010) Life-span changes of the human brain white matter: Diffusion tensor imaging (DTI) and volumetry. Cereb Cortex 20:2055–2068.

Wixted JT, Squire LR (2010) The role of the human hippocampus in familiarity-based and recollection-based recognition memory. Behav Brain Res 215:197–208 Available at: http://dx.doi.org/10.1016/j.bbr.2010.04.020.

Yassa MA, Stark CEL (2011) Pattern separation in the hippocampus. Trends Neurosci 34:515–525 Available at: https://www.sciencedirect.com/science/article/pii/S0166223611001020 [Accessed July 25, 2018].

Yau PL, Javier D, Tsui W, Sweat V, Bruehl H, Borod JC, Convit A (2009) Emotional and neutral declarative memory impairments and associated white matter microstructural abnormalities in adults with type 2 diabetes. Psychiatry Res - Neuroimaging 174:223–230 Available at: http://dx.doi.org/10.1016/j.pscychresns.2009.04.016.

Yeh FC (2021) DSI Studio. Available at: https://zenodo.org/record/4764264 [Accessed November 10, 2021].

Yeh FC, van Wedeen J, Tseng W-YI (2010) Generalized q-Sampling Imaging. IEEE Trans Med Imaging 29:1626–1635 Available at: http://ieeexplore.ieee.org/document/5432996/.

Yeh FC, Verstynen TD, Wang Y, Fernández-Miranda JC, Tseng WYI (2013) Deterministic diffusion fiber tracking improved by quantitative anisotropy. PLoS One 8:1–16.

Zhang R, Beyer F, Lampe L, Luck T, Riedel-Heller SG, Loeffler M, Schroeter ML, Stumvoll M, Villringer A, Witte AV (2018) White matter microstructural variability mediates the relation between obesity and cognition in healthy adults. Neuroimage 172:239–249.

VIII Figure Legends

Figure 1: Wanting task and subsequent Memory task. Left: Memory Encoding during Wanting Task*: Participants were asked to indicate on an 8-point-Lickert scale how much they want to have the depicted food or art image. They were previously told that they would be rewarded with the highest rated food and art image after the MRI scan.* ***Right: Memory task including target recognition and lure discrimination****: Participants had to indicate as quickly as possible if they had seen the presented food or art image in the previous task ("old"), if they had not seen it before ("new") or if it was similar to a previously seen image (also "new"). Depicted are two exemplary similar (bot not identical) food and art stimuli.*

Figure 2: Memory performance per Image Category. A) The target recognition d' and B) the lure discrimination LDI of food (F) items *(yellow)* ***is better than of non-food (NF)/art items*** *(blue). Violin plots present the distribution of the two indices over the colour-coded single subjects per image category. The estimate's CI did not include 0 which indicated an evident difference between image categories regarding d' and LDI. Estimates of all predictors and covariates are listed in Fig. 2-1 and Tables 2-1 & 2-2.*

Figure 3: Normed complexity of food and art images. *A) Normed Complexity values are not equally distributed over the two image categories. Non-Food (art) images have on average a higher normed complexity than food images. B) Response accuracy depending on normed complexity of the images.* ***Image complexity might predict response accuracy of food items.*** *The estimate of the interaction of the full model (Table 1, Eq. 3) indicated that the response accuracy of the two image categories was differently affected by normed complexity, namely food stronger than art images. Odds ratios of all predictors and covariates are listed in Fig. 3-1 and Table 3-1.*

Figure 4: Memory performance depending on subjective hunger per image category. *Actual and predicted A) target recognition d' and B) lure discrimination LDI depending on subjective hunger level per image category. Points show the actual data and lines with 95%-CI depict predictions based on full model.* ***Neither d' nor LDI were affected by the subjective hunger level.*** *The estimates of the interaction of the full model (Table 1, Eq. 6, Tables 4-1 & 4-2) indicated that the image categories were not differently influenced by hunger and the estimates of the main effect of the null model (Table 1, Eq. 7, Fig. 4-1, Tables 4-1 & 4-2)) suggested that the subjective hunger level did not affect memory performance in general. Neither task-specific hunger level (Fig. 4-3) nor ghrelin serum levels as a proxy for objective hunger (Fig. 4-4, Tables 4-3 & 4-4) predicted memory performance.*

Figure 5: Memory performance depending on wanting and image category. *A) Target recognition d' and B) lure discrimination LDI depending on wanting and image category. Depicted are mean d' (LDI) ± standard error. Predictions by the full model are depicted in Fig. 5-1.* ***Neither d' nor LDI were predicted by wanting category.*** *Estimates of all predictors and covariates are listed in Fig. 5-2 and Tables 5-1 & 5-2.*

Figure 6: Predicted response accuracy by single image wanting rating per image category. *Predictions are based on full model (Table 1, Eq. 12). The estimate of the interaction suggests that the two image categories are slightly but not evidently differently influenced by the wanting rating.* ***Higher wanting enhances response accuracy*** *as the estimate of the main effect of the full model reveals but wanting might play a more important role for the art/non-food (NF) images. Odds ratios of all predictors and covariates are listed in Fig. 6-1 and Table 6-1. Odds ratios of the wanting effect per image categorie are listed seperately in Tables 6-2 & 6-3.*

Figure 7: Predicted response accuracy by single image wanting rating for old, similar and new images respectively. *Predictions are based on full model (Table 1, Eq. 15). The estimates of the interactions endorsed the visually evident effect that* ***the wanting enhancement of the response accuracy is strongest*** *for the old images, namely* ***during memory encoding.*** *Response accuracy for new images was higher than for old images and lowest for similar images. Odds ratios of all predictors and covariates are listed in Fig. 7-1 and Table 7-1.*

Figure 8: Exemplary tracing results of in-vivo uncinate fasciculi (UF) and sub-bundles of the UF. *A: right UF with ROIs, B: left UF, C: right sub-bundle with ROIs, D: left sub-bundle. Fiber tracts are derived from deterministic tractography conducted in DSI studio (version 2022.01.11) overlaid on a subject's whole brain normalized quantitative anisotropy map. A) Regions-of-interest for tractography of the entire UF, exemplary for the right hemisphere: red: UF seed region from John Hopkins university (JHU) labels atlas (1mm), merged end region (green) consisting of Brodman Areas 11 and 47 identical to Granger et al.(2021) and Brodman area 10 from Brodman atlas (within DSI studio). C) Regions-of-interest for tractography of sub-bundle of the UF, exemplary for the right hemisphere: yellow: seed orbitofrontal cortex regions from the AAL2 atlas (within DSI studio), pink amygdala from the FreeSurferDKT subcortical atlas and violet: the entorhinal cortex from the FreeSurferDKT cortical atlas. Orientations: A: anterior, P: posterior.*

Figure 9: Memory performance depending on microstructural coherence of UF and its sub-bundle per category. *Actual and predicted A+C) target recognition d' and B+D) lure discrimination LDI depending on normalized quantitative anisotropy (nQA) of the uncinate fasciculus (UF, A&B) and its sub-bundle (C&D). Points show the actual data and lines with 95%-CI depict predictions based on full models (Table 1, Eq. 19 & Table 2, Eq. 24).* ***Neither d' nor LDI were affected by the microstructural coherence of the UF, reflected in nQA, or by its sub-bundle.*** *The estimates of the interaction of the full model indicated that the image categories were not differently influenced by the UF's microstructural coherence. The estimates of the main effect neither support an effect of microstructural coherence on memory performance (Fig. 9-1). Estimates of all predictors and covariates are visualised in Fig. 9-2 & 9-3 and listed in Tables 9-1, 9-2, 9-3 & 9-4. A hemisphere-specific role of the sub-bundle of the UF could not be confirmed (Fig. 9-4).*

Figure 10: Predicted response accuracy by wanting depending on the microstructural integrity of the UF. *Predictions are based on the full model (Table 2, Eq. 29) A) for all images and B) for old images only. The estimates of the interactions endorsed the visually evident lack of a moderation effect of nQA(UF) on the wanting enhancement of the response accuracy. Odds ratios of all predictors and covariates are visualised in Fig. 10-1 and listed in Table 10-1.*

Figure 11: Recognition accuracy of old images predicted by A) liking and B) wanting. *Depicted are predictions and their 95%-CI based on full model (Table 2, Eq. 33). The estimates of the interaction of the full model indicate that wanting and liking affect both image categories similarly. The enhancement by wanting during memory encoding is slightly stronger than by general liking. Odds ratios of the corresponding models are listed in Tables 11-1 & 11-2.*

Figure 12: Response accuracy predicted by calorie content of the food items*. Predictions are based on the null model 1 (Table 2, Eq. 37). Mean predictions and their 95%-CI are depicted. Calorie content does not evidently influence response accuracy of the food images. Odds ratios of all predictors and covariates are visualised in Fig. 12-1 and listed in Table 12-1.*

Figure 13: Memory performance per gender group. *A) The* ***target recognition d' and B) the lure discrimination LDI of female (F) participants*** *(bordeaux)* ***is better than of male participants (M)*** *(orange). Violin plots present the distribution of the two indices per gender. The estimate's CI did not include 0 which indicated an evident difference in memory performance between gender groups.*

Figure 14: Memory performance depending on personality trait neuroticism. *Actual and predicted A) target recognition d' and B) lure discrimination LDI depending on neuroticism assessed with the NEO-FFI. Points show the actual data and lines with 95%-CI depict predictions based on null model 2 (Table 2, Eq. 41). d' and LDI were evidently predicted by neuroticism.* ***The more neurotic the participants, the worse their memory performance.*** *Estimates of the corresponding models are listed in Tables 14-1 & 14-2.*

Figure 15: Microstructural coherence of UF depending on age and gender. *Actual and predicted microstructural coherence of the UF, reflected in its nQA value, A) by age and B) by gender. Points show actual data of the colour-coded subjects. A) Prediction line with 95%-CI is based on null model 2 (Table 2, Eq. 45). B) Violin and boxplots present the distribution of the nQA values over both genders.* ***Neither age nor gender predicted the microstructural coherence of the UF.*** *Odds ratios of the corresponding models are listed in Tables 15-1. The effects of age and gender on the whole brain's microstructural coherence is shown in Fig. 15-1.*

IX Table Legends

Table 1: Model equations of full and null models and the difference in predictive accuracy.

Table 2: Model equations of full and null models and the difference in predictive accuracy.

Table 3: Mean, standard deviation and range of normalized quantitative anisotropy values (nQA) of the uncinate fasciculus (UF) and its sub-bundle as well as the whole brain

X Extended Data Legends

Figure 2-1: Model estimates of the full model for the effect of image category and covariates (Table 1, Eq. 1) on d' and LDI. Values indicate the positive (blue) or negative (red) mean estimate of the posterior distribution and whiskers represent the 50% (thick, inner) and 95% (thin, outer) CI. The effect of image category (F>NF) and Gender (M<F) on memory performance measures seems to be evident as their 95% CI do not include Zero.

Table 2-1: Full and null Bayesian linear regression models for the effect of image category on d'.

Table 2-2: Full and null Bayesian linear regression models for the effect of image category on LDI.

Figure 3-1: Model estimates of the full model for the effect of normed complexity, image category and covariates (Table 1, Eq. 3) on response accuracy. Values indicate the positive (blue) or negative (red) median odds ratio (exponentiated regression coefficients) and whiskers represent the 50% (thick, inner) and 95% (thin, outer) CI. The interaction of image category with normed complexity as well as the effect of image category (F>NF) and Gender (M<F) on response accuracy seem to be evident as their 95% CI did not include Zero.

Figure 9-3: Model estimates of the full model (Table 2, Eq. 24) for the effect of microstructural properties of the sub-bundle of the UF and covariates on d' and LDI. Values indicate the positive (blue) or negative (red) mean estimate of the posterior distribution and whiskers represent the 50% (thick, inner) and 95% (thin, outer) CIs. The sub-bundle of the UF, which connects OFC and MTL, neither moderated effects of wanting category, subj. hunger level or image category on memory performance, nor predicted its microstructural coherence d' or LDI. Only the effect of Gender (M<F) on memory performance measures seems to be evident as its 95% CI do not include Zero.

Table 9-1-1: Full and null (1-6) Bayesian linear regression models for the effect of microstructural coherence of the UF on d'.

Table 9-1-2: Null (7-14) Bayesian linear regression models for the effect of microstructural coherence of the UF on d'.

Table 9-2-1: Full and null (1-6) Bayesian linear regression models for the effect of microstructural coherence of the UF on LDI.

Table 9-2-2: Null (7-14) Bayesian linear regression models for the effect of microstructural coherence of the UF on LDI.

Table 9-3-1: Full and null (1-6) Bayesian linear regression models for the effect of microstructural coherence of the sub-bundle of the UF on d'.

Table 9-3-2: Null (7-14) Bayesian linear regression models for the effect of microstructural coherence of the sub-bundle of the UF on d'.

Table 9-4-1: Full and null (1-6) Bayesian linear regression models for the effect of microstructural coherence of the sub-bundle of the UF on LDI.

Table 9-4-2: Null (7-14) Bayesian linear regression models for the effect of microstructural coherence of the sub-bundle of the UF on LDI.

Figure 9-4: Memory performance depending on microstructural coherence of left and right sub-bundle of UF. Actual and predicted A+B) target recognition d' and C+D) lure discrimination LDI depending on normalized quantitative anisotropy (nQA) of the A+C) left and B+D) right sub-bundle of the UF. Points show the actual data and lines with 95%-CI depict predictions based on null models (cf. Table 2, Eq. 25). Neither d' nor LDI were affected by the microstructural coherence of a hemisphere-specific sub-bundle of the UF.

Figure 10-1: Odds ratios of the full model (Table 2, Eq. 29) for the effect of microstructural properties of the UF and covariates on response accuracy. Values indicate the positive (blue) or negative (red) mean estimate of the posterior distribution and whiskers represent the 50% (thick, inner) and 95% (thin, outer) CIs. The UF neither moderated effects of wanting category, subj. hunger level or image category on memory accuracy, nor predicted its microstructural coherence memory accuracy. Only the effect of Gender (M<F) on memory accuracy seems to be evident as its 95% CI do not include Zero.

Table 10-1: Full and null Bayesian linear regression models for the moderation effect of the microstructural coherence of the UF on single image wanting regarding response accuracy.

Table 11-1: Full and null Bayesian linear regression models for the effect of single image liking ratings of previously encoded (old) images on response accuracy.

Table 11-2: Full and null Bayesian linear regression models for the effect of single image wanting ratings of previously encoded (old) images on response accuracy.

Figure 12-1: Odds ratios for the effect of calorie content of food images on response accuracy: A) null model 1 (Table 2, Eq. 37), B) full model 1 (Table 2, Eq. 36). Values indicate the positive (blue) or negative (red) median odds ratio (exponentiated regression coefficients) and whiskers represent the 50% (thick, inner) and 95% (thin, outer) CI. A) Calorie content did not evidently predict food memory accuracy. B) Additionally, the wanting enhancement of memory accuracy was not different between calorie quartiles. Only the better memory accuracy for new images and the effect of gender seem to be evident as their 95% CI did not include Zero.

Table 12-1: Full and null Bayesian linear regression models for the effect of calorie content on food memory accuracy.

Table 14-1: Full and null Bayesian linear regression models for the effect of neuroticism on d'.

Table 14-2: Full and null Bayesian linear regression models for the effect of neuroticism on LDI.

Table 15-1: Full and null Bayesian linear regression models for the effect of age and gender on microstructural coherence of the UF.

Figure 15-1: Microstructural coherence of whole brain depending on age and gender. Actual and predicted microstructural coherence of the whole brain, reflected in its nQA value, A) by age and B) by gender. Points show actual data of the colour-coded subjects. A) Prediction line with 95%-CI is based on null model 2 (Table 2, Eq. 45). B) Violin and boxplots present the distribution of the nQA values over both genders. Neither age nor gender predicted the microstructural coherence of the UF.

View publication stats